EFFECTS OF BIODIESEL COMBUSTION PRODUCT ON ENGINE WEAR PERFORMANCE OF LUBRICANT

PRASIT WATTANAWONGSAKUN

A THESIS SUBMITTED IN PARTIAL FULFILLMENT

OF THE REQUIREMENT FOR THE DEGREE OF

MASTER OF ENGINEERING IN AUTOMOTIVE ENGINEERING

(INTERNATIONAL PROGRAM)

INTERNATIONAL COLLEGE

KING MONGKUT'S INSTITUTE OF TECHNOLOGY LADKRABANG

2011

KMITL-2011-IC-M-004-014

Thesis	Effects of Biodiesel Combustion Product on Engine Wear Performance of Lubricant
Student	Mr. Prasit Wattanawongsakun
Student ID.	50061903
Degree	Master of Engineering
Program	Automotive Engineering (International Program)
Year	2012
Thesis Advisor	Assoc. Prof. Dr. Chinda Charoenphonphanich

ABSTRACT

Currently, the problems of petroleum pricing and supply-chain structure are a pressing issue in many countries. One of the solutions is to switch to an alternative fuel derived from agricultural products. In Thailand, a recent trend of alternative fuel has inclined towards biodiesel despite results from various studies indicating that some properties of biodiesel fuel itself could have negative effects on the engine system such as acid value, oxidation stability, etc. Nonetheless, a study on the effect of biodiesel combustion products on wear performance of contaminated lubricant is still limited. Therefore, such topic is the main objective of this study.

One of the major causes of diesel engine wear is lubrication oil contaminated with combustion products. The combustion products usually occurred from an incomplete combustion process in an engine. Combustion products could deposit at the interface between the piston and cylinder. There has been suggested in literature that this might result in a breakdown of lubricant oil film, permitting a direct contact between combustion products and surfaces of those engine parts.

The present study was conducted on a laboratory scale, using 2 small diesel engines which were generally used in agricultural activities. The testing comprised of 2 seperated setups in which diesel fuel and biodiesel fuel was employed to operate each engine. After running the test engines according to a set of desired conditions, lubricant oil samples from each engine were collected for further laboratory experiments. A portion of collected lubricants was used to qualitatively compare wear performance by using ball-on-flat Micro-Tribometer. The rest of

collected samples were chemically analyzed by techniques such as FT-IR, ICP to examine the lubricant conditions after the engine tests.

Overall results obtained from all the experiments suggested that both fuel could have a significant influence on reducing an anti-wear performance of engine lubricant especially after running the test engines under controlled full-load for 200 hours. A large amount of soot contamination from diesel combustion led to a significant increase of lubricant effective viscosity. This could prevent a proper flow of lubricant into the contact area resulting in poor lubricated conditions. Furthermore, while considerable amount of soot contamination was also found in lubricant sample tested with biodiesel, an evidence of biodiesel (ester-group) contamination in tested lubricant was also substantial. Such contamination could possibly result in a reduction of effective viscosity and was believed to be the main reason for worse wear performance by engine running with biodiesel. However, which type of fuel, or more precisely, which type of combustion-product contamination has more detrimental effect to an engine wear was still not clear under the current study.

ACKNOWLEDGEMENT

This thesis could not be completed without the assistance of many persons to whom I would like to express my sincere appreciation.

First, I would like to sincerely thank my advisor, Dr. Chi-na Benyajati, who has given me many helpful suggestions, useful advice and fruitful discussions during the undertaken research.

I would also like to sincerely thank Asst. Prof. Dr. Chinda Charoenphonphanich for kind advising and helping, and Assoc. Prof. Dr. Kosaka Hidenori for the suggestions.

Moreover, I would like to sincerely thank Assoc.Prof. Dr. Surapol Raadnui from KMITNB, who has given me many helpful suggestions about my experimental. And I would also like to sincerely thank Assoc. Prof. Dr. Siriluck Nivitchanyong for the suggestions and discussions. I would like to show gratitude to National Metal and Materials Technology Center (MTEC), especially the automotive laboratory for providing the laboratory equipments and instruments as well as financial supporting.

I am grateful to National Science and Technology Development Agency (NSTDA), which provided the full scholarship for studying in the master program.

Special thanks go to MTEC's laboratory: Vibrational Spectroscopy Lab (Spectroscopy Lab 2), Polymer Physics Lab (Rheology Lab) and Bioenergy Lab (Bioenergy Lab 1) for helping me during the experiment.

Prasit Wattanawongsakun

TABLE OF CONTENTS

TABLE OF CONTENTS (CONT.)

LIST OF TABLES

LIST OF FIGURES

LIST OF FIGURES

CHAPTER 1

INTRODUCTION

1.1 Significance and Background

Currently, the anticipated problem of petroleum insufficiency in the near future is the most important concern in global scale. Furthermore, the problem of petroleum price is a pressing issue in many countries. Thus, developments of alternative energy are an attractive research topic.

A research on an effect of biodiesel burning residuals on the performance of lubricant is one of areas to investigate the advantages and disadvantages of using biodiesel as a fuel. There has been many studies in Thailand involving the use of biodiesel in engines. Several engine problems have been reported with suggestions made regarding the relating properties of biodiesel as shown in Table 1.1.

Table 1.1 Engine general problems related to biodiesel's properties

General Problem	Related Biodiesel's Properties
Fuel system corrosion and rubber parts swell	Acid Value, Methanol, Oxidation Stability, Ester
Fuel pump damaged or fuel filter clogged	Oxidation Stability, Ester, Glyceride, Water, Low Temperature
Properties of biodiesel change when leaving for long time	Acid Value, Oxidation Stability, Water, Low Temperature
Piston rings adhered to liner, injector clogged, lubrication oil contaminated with combustion products	Acid Value, Ester, Glyceride, Water

1.2 Objective

The objective of the study was to carry out a qualitative study about impact of biodiesel fuel application in Thailand focusing on engine parts wear. The effects of biodiesel combustion product on engine wear performance of lubricant was the main interest of this study.

1.3 Scopes

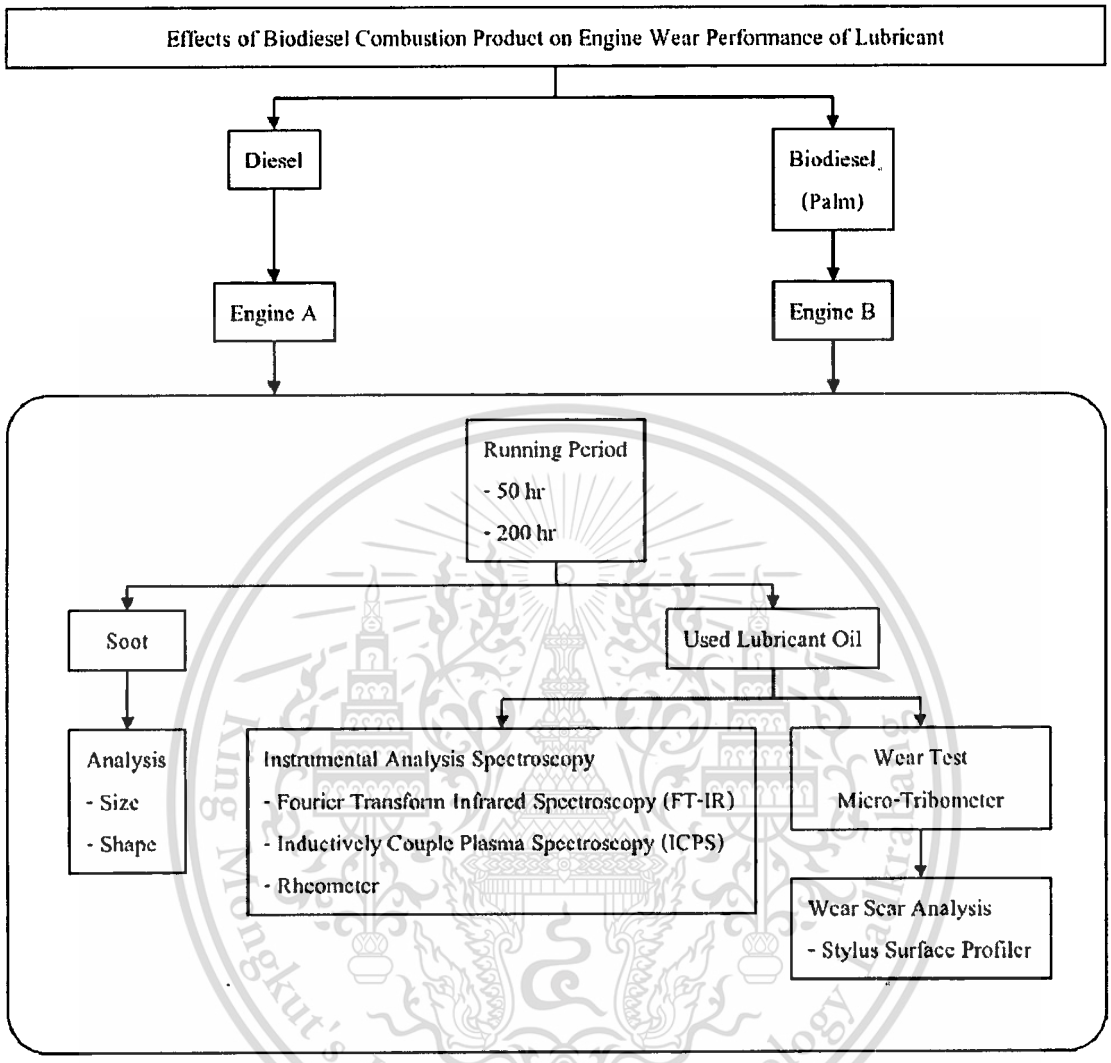

Figure 1.1 Research layout on the study on the effect of biodiesel combustion product on engine wear performance of contaminated lubricant

1.4 Expected Benefits

The expected benefits from this research were the results of contamination in lubricant oil after a use in a diesel engine. The results could then be used to understand the condition of engine wear for both diesel and biodiesel fuel.

CHAPTER 2

LITERATURE REVIEWS

2.1 Previous Study

The five major wear mechanisms in a diesel engine are abrasion, adhesion, fatigue, corrosion and lubricant breakdown. Corrosion and lubricant breakdown involves a series of chemical reactions that lead to wear while abrasion, fatigue, and adhesion involve mechanical damage of surface. For all above five forms of wear, lubricant contamination is predominant driver for wear.

Currently, the alternative fuel is an interesting issue in Thailand. Raadnui et al. [1] reported that pure refined palm oil (RPO) and RPO blended fueled engines were wearing at a normal rate when compared with conventional diesel fuel.

Combustion products-contaminated lubrication oil is one of the causes for diesel engine wear. Diesel soot could interfere with the lubricating oil thereby leading to increased wear and increasing viscosity of lubrication oil [2].

There are various types of wear testing devices that have been reported in published literature. For wear measurements, it is very important to decide the variables that need to be controlled, ignored, and measured. The significant variables in the friction and wear process are: load, velocity, temperature, contact area, geometry, and surface finish [2]. Load plays a very significant role in wear testing as it directly influences the surface temperature and can affect the real contact area. However, most wear experiments are performed at relatively low loads while the limitation are imposed by a need for more rugged equipment and higher power requirement.

Many authors have disputed the adsorption theory proposed by Rounds. Ryason et al. [3] who performed wear tests on a ball-on-flat-disk tribometer using carbon black and steel balls made of AISI 52100 steel. Wear tests were performed on oil added with carbon black, alumina and silica. Investigations were carried out on the wear scars from the tests using scanning electron microscope (SEM) and electron probe micro-analysis. The SEM pictures showed that the scars on the surfaces of the balls worn in the presence of oils containing carbon black, alumina and silica were similar, and differ from that of the ball worn in the presence of oil alone. Ryason concluded that the wear that occurred was abrasive in nature.

Berbeizer et al. [4] investigated the role of carbon black on mild lubricated wear. The test setup they used involved a plane-on-plane tribometer to simulate lubricated mild wear between ring, cylinder and particles in suspension. They conducted a systematic study of carbon black parameters on mild wear by evaluating special test blends in which different types of commercial carbon black were used as model compounds. They concluded that bore polishing was influenced more by the size, nature, and concentration of carbon black rather than by the products of oil degradation. They suggested that decreasing the amount of carbon black reaching the piston or suspension in the lubricant could reduce bore polishing.

Gautam et al. [5] showed the wear increased with higher soot concentration and decreased with higher phosphorous level. The effect of dispersant level was not significant, although on average, higher dispersant level reduced wear. The effect of sulfonate substrate was not evident in this range of concentrations. They concluded the average wear from soot contaminated lubrication oils were higher than the average worn without soot contamination. Diesel soot reduces the oil's anti-wear properties, possibly by an abrasive wear mechanism. They used ball-on-flat-disk tests performed with soot and alumna showed comparable wear ratio. Since alumina was a known abrasive, it might infer that soot act as an abrasive causing either actual metal abrasion or just abrasion of the anti-wear film resulting in metal-to-metal contact. The soot contaminated the lubricant and changed the chemical properties resulting in the lubricant ceasing to perform its function. This caused an increase in viscosity of the engine oil causing pump ability problems [6].

Yamaguchi et al. [7] used two fully formulated PC-9 diesel engine oils, A and B for a bench test study. The two oils were identical as the level and type of zinc dialkyl dithiophodphate (ZDDP) and detergents used, but differed in the dispersants and viscosity index (VI) improvers used. The fresh oil A and B had viscosity behavior and total base number: Oil A viscosity, 14.8 cSt and total base number, 10.069 mg KOH/g. Oil B viscosity, 15.43 cSt and total base number, 10.009 mg KOH/g. The results of the two engine test were that oil B clearly showed higher wear than oil A after the 300 hours test. The percentage of soot in the oil at the end of tests was comparable; in fact, the good oil had a slightly higher amount of soot.

Exhaust gas recirculation (EGR) is one of the effective means to reduce the NOX emission from diesel engines. Aldajah [8] showed EGR did accelerate the degradation of engine oil in

terms of increased soot particulate loading (7-12% compared to about 4% without EGR) and increased acid content (TAN) by two to three times.

Song et al. [9] discussed that the initial structure alone did not dictate the reactivity of diesel soot and rather the initial oxygen groups had a strong influence on the oxidation rate. A comparison of the complete oxidation behavior and burning mode was made to address the mechanism by which biodiesel soot enhances oxidation. Diesel soot derived from neat biodiesel (B100) was far more reactive during oxidation than soot from neat Fischer-Tropsch diesel fuel (FT100). B100 soot underwent a unique oxidation process leading to capsule-type oxidation and eventual formation of grapheme ribbon structures. The results demonstrated the importance of initial properties of the soot, which led to differences in burning mode. Incorporation of greater surface oxygen functionality in the B100 soot provided the means for more rapid oxidation and drastic structural transformation during the oxidation process.

Biodiesel engine tests were conducted and the engine performance and emission comparisons were made with an ultra-low sulphur diesel fuel by Zheng et al. [10]. A naturally-aspirated four-stroke single-cylinder DI diesel engine was instrumented for tests. For the investigated conditions, the test resulted in the high load operating condition, the engine-out NOX emissions were dependent on the fuel cetane number, for the same start of injection. The biodiesel fuel with a cetane number similar to the diesel fuel produced higher NOX emissions than the diesel fuel. The biodiesel fuels with a higher cetane number, however, had comparable NOX emissions with the diesel fuel. A higher cetane number would result in a shortened ignition delay period thereby allowing less time for the air/fuel mixing before the premixed burning phase. Consequently, a weaker mixture would be generated and burnt during the premixed phase resulting in relatively reduced NOX formation. Generally the emissions of soot, CO and total hydrocarbon were lower for the engine fuelled with biodiesel.

While biodiesel possesses many similarities to conventional diesel fuel, biodiesel possesses many unique properties that need to be considered for its application in current and emerging engine technologies. Biodiesel can increase NOX emissions in engines with pump-line-nozzle fuel systems due to its elevated bulk modulus of compressibility, a feature of soybean oil-derived biodiesel that primarily is used in the United States. That biodiesel also can yield a NOX increase in common rail engines cannot be explained by the difference in compressibility, and remains an open question for research. However, this NOX effect can be circumvented successfully by

additization with cetane improver, shifting the methyl oleate concentration in the biodiesel fuel, or shifting the injection timing to compensate for the advance caused by the fuel. Biodiesel, like other oxygenated diesel fuels, can reduce the amount of soot formed in the diesel spray flame and can lead to reduced total particulate emissions. However, as has been reported, ester molecular structures, such as the methyl that comprise biodiesel, are less effective soot suppressants than ether structures [11].

The Joint Oil Analysis Program Technical Support Center (JOAP-TSC) evaluated FT-IR spectroscopy as the appropriate technology to meet advanced physical property test requirements [12].The JOAP method differs from the reference method in that it provides absolute value for components of the oil. The method involves the subtraction of an empty cell background from the used oil spectrum. Characteristic regions from the resulting spectrum are used to determine used oil parameters and components. It is critical to collect large amounts of data to obtain a representative picture of typical contamination and degradation levels and their effect on the FT-IR spectrum.

The investigation of the effect of different concentrations of palm oil diesel contaminated lubricant on the wear characteristics of cast irons against mild steel shows: The use of pure commercial lubricant resulted in a moderate wear rate, whilst pure palm oil diesel lubricant produced the highest wear rate compared with the other combinations of contaminated lubricants [13]. A comparative study of wear, friction, viscosity, lubricant degradation and exhaust emissions was carried out a palm oil and mineral oil-based commercial lubricating oil. The results demonstrated that the palm oil based lubricating oil exhibited better performance in terms of wears, and that the mineral oil based lubricating oil exhibited better performance in terms of friction. However, the palm oil based lubricant was the more effective in reducing the emission levels of CO and hydrocarbon [14].

A review on biodiesel production, combustion, emissions and performance by Syed Ameer Basha, K. Raja Gopal, and S. Jebaraj can concluded: Even though 350 oil-bearing crops are identified, only few are potential biodiesel like sunflower, rapeseed, palm and jatropha. It is observed that biodiesel has similar combustion characteristics as diesel and also found that the base catalyst performs better than acid catalyst and enzymes. It is also inferred that the engine performance was inferior when using vegetable oil/ diesel blend as the high viscous oil caused injector coking and contaminated the lubricating oil. The tests with refined oil blends indicated

considerable improvement in performance. The emission of unburnt hydrocarbon from the engine was found to be more on the all the fuel blends as compared to diesel. The emission of oxides of nitrogen from the engine found to be higher on the all fuel blends as compared to diesel [15].

Lubricant oil which is fuel-diluted with biodiesel, which is known to contain unsaturated hydrocarbon bonds, would be expected to be more prone to oxidation. Current diesel engines designed to meet environmental standards tend to introduce more soot into the crankcase oil. The new diesel engine oils for use with biodiesel fuel must be capable of dispersing soot to minimize soot-induced viscosity increase of the oil and prevent engine wear. Lubricant oils will also need improved oxidation and corrosion inhibition. A study by Tze-Chi Jao et al. using B20 fuel showed that passing engine test data was obtained for soot-induced viscosity thickening, oxidation and wear, however, deposits increased and oxidation increased significantly when using biodiesel fuel-diluted engine oil [16].

A study on tribology of soot suspension by Hiralal Bhowmick, S K Majumdar and S K Biswas [17] investigated the influence of physical and chemical properties of soot particles on the friction and wear of mating components. They concluded that if the soot was strongly graphitic the friction and wear were moderate. However, if the soot was made of chemically active organic groups, the friction and wear were high. The grafting of the surfactant on the soot particles was found to have a profound effect on the dispersion of the soot, in general, while, between the different soot types, the tribology characteristic was differentiated by their physical structures and chemistry.

2.2 Inductively Coupled Plasma Spectroscopy (ICPS) [18]

ICPS is the methods for quantity analysis of metals and non-metals in solution of samples. The solution of sample is converted into small droplets (aerosol) with Nebulization through the peristaltic pump shown in Figure 2.1 into the plasma of the ICP torch. The solution of samples obtains a high energy to the decay of the atom. The atom is stimulated to the excited and partly into ions in the process called the atomization and Ionization of atoms. The stimulated ions would emit light which has specific wavelength. The emitted light will pass into the spectrometer and only the required wavelength of the light element analysis will be used to detect for the signal

which is related to the concentration of the solution. The data collection and processing is controlled by computer as shown in Figure 2.2.

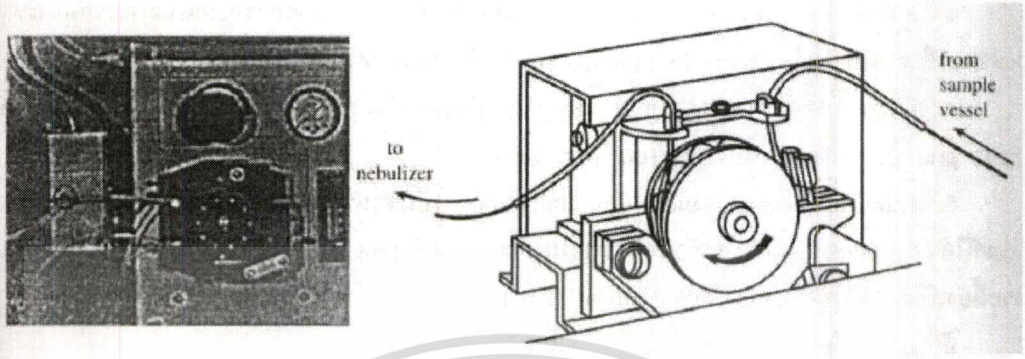

Figure 2.1 Peristaltic pump in ICPS

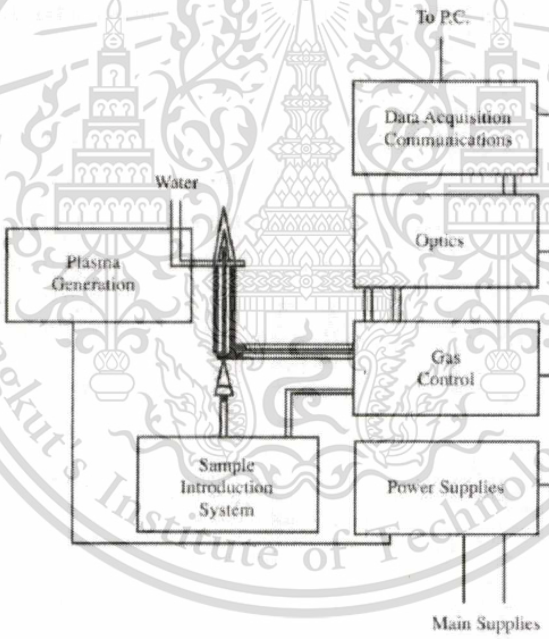

Figure 2.2 Important components of ICPS

2.3 Fourier Transform Infrared Spectroscopy (FT-IR) [18]

Figure 2.3 Fourier Transform Infrared Spectroscopy (FT-IR)

Infrared spectroscopy is a technique used to analyze and study the structure of the molecules in both solid, liquid or gas by studying the transition series of vibration or rotation of the functional groups of the molecules caused by the absorption of the infrared spectrum of the molecule. It is a measure of the infrared absorption spectrum of the transition series of the oscillations of the molecules and affects the vibration of molecular bonds. The infrared spectrum is a spectrum plot of the number of waves (wavenumber, $\bar{\nu}$) has units in per centimeter (cm^{-1}) or frequency (Hz) with the infrared absorbance or % T.

In the analysis of infrared spectra of the samples, the detection of the vibration or the peak of the functional groups in the primary structure of the compounds that may appear in the spectrum is important, for example, the functions of C=O, O-H, N-H, C-O, C=C, C≡C, C≡N and NO2 can detect the main information of the structure immediately. It does not need to analyze the vibration of C-H at 3000 cm^{-1} wave number and the implementation of the following topics, respectively.

1. Check concentration of Carbonyl (C=O).
   - Peak of the C=O group appears at 1820-1660 cm^{-1} range and the absorption maximum.

2. In the case of C=O groups to check for the following functional groups (If have not C=O groups, proceed in accordance with Article 3).
   - In the case of acid, to detected the -OH group by detect a broad peak appears in the 3400-2400 cm^{-1} overlap with the peak of -CH.
   - In the case of amide, to detected the -NH group with a medium height near 3400 cm^{-1}, and sometimes can detect 2 peaks by the second peak is height only half of the peak one.
   - In the case of ester, to detected the C-O group appears at the peak of the absorption of light is much closer to 1300-1000 cm^{-1}
   - In the case of anhydride, to detected two peaks of C=O at 1810 and 1760 cm^{-1}
   - In the case of aldehyde, to detected 2 peaks of –CH group at the very low absorption near 2850 and 2750 cm^{-1} peak to the right of aliphatic CH.
   - In the case of ketones are not detected at the peak of oscillations from the functional groups of the amide, esters, anhydride or aldehyde acid.

3. If the samples have not C=O group, to check for the following function
   - In the case of alcohol, to detected the –OH or phenol at the large peak near 3400-3300 cm^{-1}, and appearance of the C-O peak near 1300-1000 cm^{-1}
   - In the case of amine, to detected the –NH group appear the average peak near 3400 cm^{-1}
   - In the case of ether, to detected the C-O group near 1300-1000 cm^{-1} but not appear the –OH peak near 3400 cm^{-1}

4. If the samples is double bond and/or aromatic rings
   - In the case of C=C, to detected the peak light absorption (w) near1650 cm^{-1}
   - In the case of aromatic rings, to detected a medium to high peak in the range 1600-1450 cm^{-1}
   - Confirm the samples is double bond or aromatic rings by detected the C-H group in the range of 3000 cm^{-1}
   - In the case of aliphatic C-H, to detected the number of wave short more than 3000 cm^{-1}

5. Triple bond
   - Detected a high peak near 2250 cm^{-1}
   - Detected an obvious small peak near 2150 cm^{-1} and detected the acetylenic C-H near 3300 cm^{-1}

6. In the case of Nitro group, to detected high 2 peaks near 1600-1530 cm^{-1} and 1390-1300 cm^{-1}

7. In the case of Hydrocarbon group, there is not identified but confirmed by the peak of absorption of C-H at range 3000 cm^{-1}

When using the process of structural analysis shown above in conjunction with data from Figure 2.4 and Table 2.1, the vibration of the functional groups of compounds could be determined in the infrared spectrum format indicating the compounds of the test sample.

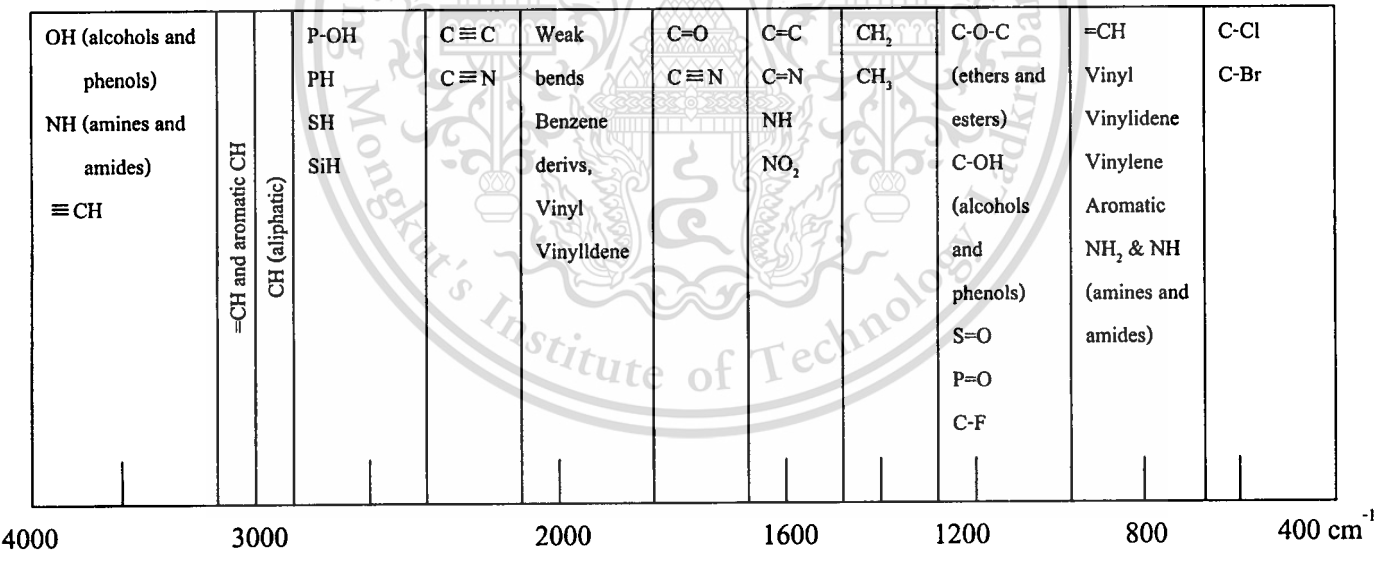

Figure 2.4 Vibration of the functional groups of infrared spectrum

Table 2.1 The wave region of the functional groups of possible presenting compounds

Region	Group	Possible Compounds Present
3700-3100	-OH	Alcohols, aldehydes, carboxylic acids
	-NH	Amides, amines
	≡C-H	Alkynes
3100-3000	=CH	Aromatic compounds
	$-CH_2$ or –CH=CH-	Alkenes or unsaturated rings
3000-2800	-CH, $-CH_2-$, $-CH_3$	Aliphatic groups
2800-2600	-CHO	Aldehydes (Fermi doublet)
2700-2400	-POH	Phosphorus compounds
	-SH	Mercaptans and thiols
	-PH	Phosphines
2400-2000	-C≡N	Nitriles
	$-N=N^+=N^-$	Azides
	-C≡C-	Alkynes
1870-1650	C=O	Acid halides, aldehydes, amides, amino acids,
		Anhydrides, carboxylic acids, esters ketones, lactams,
		Lactones, quinones
1650-1550	C=C, C=N, NH	Unsaturated aliphatics, aromatics, unsaturated
		Heterocycles, amides, amines, amino acids
1550-1300	NO_2	Nitro compounds
	CH_3 and CH_2	Alkanes, alkenes, etc.
1300-1000	C-O-C and C-OH	Ethers, alcohols, sugars
	S=O, P=O, C-F	Sulfur, phosphorus, and fluorine compounds
1100-800	Si-O and P-O	Oganosilicon and phosphorus compounds
1000-650	=C-H	Alkenes and aromatic compounds
	-NH	Aliphatic amines
800-400	C-halogen	Halogen compounds
	Aromatic rings	Aromatic compounds

CHAPTER 3

EXPERIMENTAL DESIGN

3.1 Design of test

3.1.1 Engine

In Thailand, Kubota has the highest marketing share for a one-cylinder agricultural engine. The KUBOTA RT140PLUS-ESE engines are designed as a power drive for many agricultural assemblies. The engine specifications are given in Table 3.1.

Table 3.1 Test engine specifications

Description	Technical data
Code	Kubota RT140DI PLUS-ESE
Type	Diesel Direct Injection/Single horizontal piston/Water cooling system
Cylinder diameter x Stroke, mm. x mm.	97 x 96
Displacement Volume, mm^3	709
Max. Power, hp at rpm	14/2,400 (10.3kw/2,400)
Continuous Power, hp at rpm	12.5/2,400 (9.2kw/2,400)
Specific fuel consumption rate (at continuous power), g/hp.hr	170 (231 g/kw.hr)
Compression ratio	18:1
Max. Torque, kgf.m at rpm	5.0/1,600
Cooling water system volume, dm^3(liters)	2.1
Fuel tank volume, dm^3(liters)	11
Lubrication system volume, dm^3(liters)	2.8
Engine weight, kg	112

3.1.2 Load conditions

The load provided for the experimental was a single-phased A.C. synchronous generator. The maximum output was 10 kw 230 Voltage at rotational speed of 1500 rpm. 4 V-belt

B type were used for translating an engine power to the generator. The engine and generator pulley size was 4 and 7 inches respectively as shown in Table 3.2 and Figure 3.1.

Table 3.2 Single phase A.C. synchronous generator specification

Description	Value
Speed (rpm)	1500
Output (kw)	10
Current (A)	
- Series connection	43.5
- Parallel connection	87
Voltage (V)	
- Series connection	230
- Parallel connection	115
Pole number	4
Power factor	1

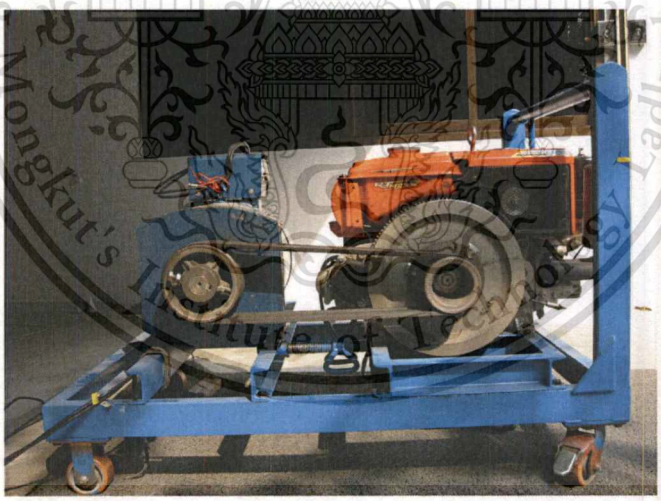

Figure 3.1 A.C. generator connected with test engine

The wire connection from the generator to a spotlight loading unit is shown in Figure 3.2 and Figure 3.3. The spotlight loading unit was used to control the load by switching the desired spotlight on/off. There were 6 of 300, 500, 1000, 1500 watt spotlights installed on the loading unit. The condition of loading was a full throttle of engine speed about 2000 rpm and max

speed of generator 1500 rpm with the real output about 7500 watt 30 ampere 230 voltage. The experimental would be carried out on the engines with the controlled payload for a duration of 50 and 200 hours with each different fuel.

Figure 3.2 Spotlight loading unit

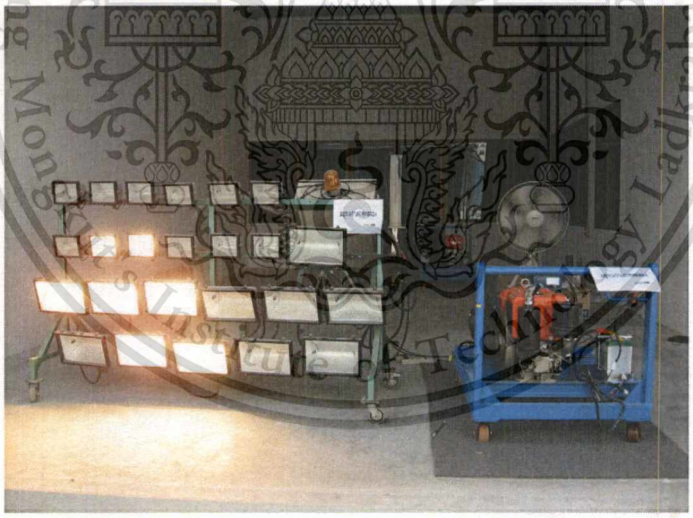

Figure 3.3 Overall engine test arrangement

3.2 Experimental technique

3.2.1 Description of lab-scaled test rig

The micro tribometer was used in this research. Generally, it was a ball-on-flat testing machine as shown in Figure 3.4 and Figure 3.5.

Specification

- Radius of Ball Steel 6.35 mm.
- Applied Load 200 N
- Stroke 10 mm.
- Oscillates Frequency 10 Hz.
- Duration time 33 min 20 sec (ball displacement 400 m.)
- Temperature 80 °C
- Humidity 40-60 %

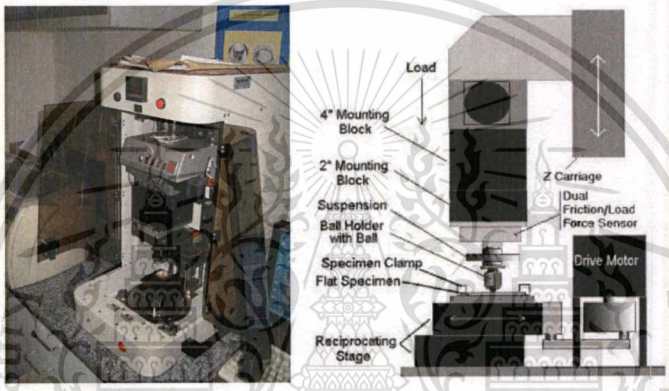

Figure 3.4 Ball-on-Flat tribometer testing machine

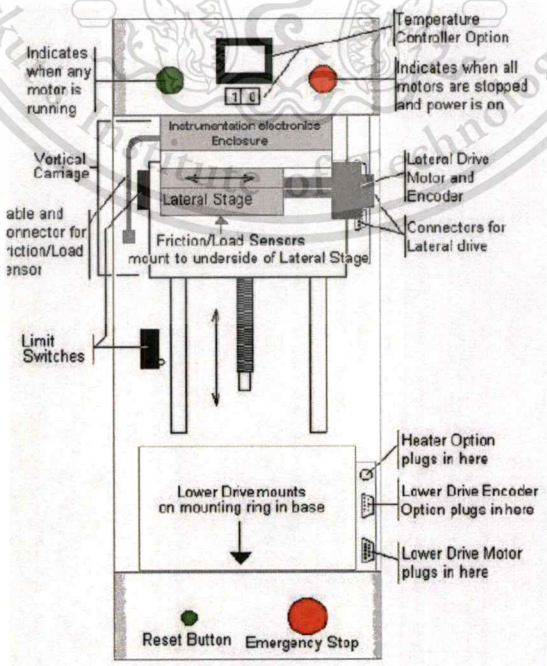

Figure 3.5 Tribometer components

3.2.2 Test specimens

The specimens were prepared from a cylinder wall (Liner) sectioned by a wire-cut machine to pieces with geometries as shown in Figure 3.6.

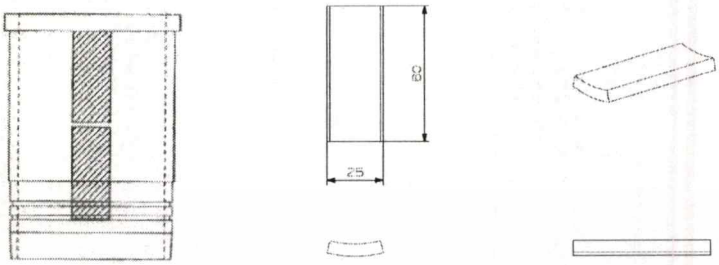

Figure 3.6 Specimens dimension for Tribometer testing

3.2.3 Fuel

A sample of biodiesel was tested as-received according to the announcement of department of energy to analyze the general quality of the acquired fuel before using in the engine test as shown in Table 3.3.

Table 3.3 Pre-test analysis of as-received biodiesel properties

Properties, Unit	Department of Energy Business of Thailand Announcement	Value	Method
Methyl Ester Content, %wt.	≥96.5	98.86	EN 14103
Density at 15°C, kg/m^3	860-900	875	ASTM D 1298
Viscosity at 40°C, cSt	3.5-5	4.454	ASTM D 445
Flash Point, °C	≥120	162	ASTM D 93
Carbon Residue, %wt	≤0.30	0.01	ASTM D 4530
Water Content, %wt	≤0.050	0.0311	EN ISO 12937
Oxidation Stability at 110°C, hour	≥10	16.39	EN 14112
Acid Value, mg KOH/g	≤0.50	0.17	ASTM D 664
ASTM Color	-	0.80	ASTM D 1500/156
Gross Heat, MJ/kg	-	39.60	ASTM D 240
Cloud Point, °C	-	15.80	ASTM D 2500
Pour Point, °C	-	12	ASTM D 97

From the analysis results, the important biodiesel property was an oxidation stability at 110°C which must not be lower than 10 hours. This value would indicate the chance of biodiesel property changing from a preservation during the whole study.

3.2.4 Lubricants

The lubricant oil sample was collected by draining from the engine reservoir after the two different continuous engine test durations of 50 hours and 200 hours under 75% work load for each fuel. The properties of fresh lubricant oil are displayed in Table 3.4.

Table 3.4 Properties of fresh lubricant oil

Type	PTT V-120 Diesel Engine Oil API CC/SD SAE40
Viscosity @ 100 °C, cSt	15.0
Viscosity Index	98
Flash Point, (COC), °C	270
Total Base Number, mg KOH/g	4.4

3.2.5 Specimen inspection

A stylus-type machine shown in Figure 3.7 was employed to measure surface roughness profiles of liner specimens before and after tribometer testing.

Figure 3.7 Roughness measurement machine

Additionally, the surface hardness of the specimen was examined with the Universal Hardness Testing Machine shown in Figure 3.8. The Rockwell HRC scale was used. The obtained results were averaged for a selection of appropriate ball steel counterface in Micro-Tribometer tests. It was required that the surface in contact with the cylinder wall specimen should have a higher hardness value than that of the cylinder wall (Liner) in order to limit the wear to occur mainly on the specimen surface during the test.

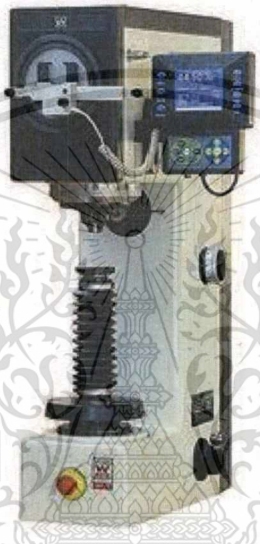

Figure 3.8 Universal Hardness Testing Machine (Instron Model 930/250)

Figure 3.9 shows hardness measurement locations of the liner specimens. There were 6 measurement points evenly separated along the centerline of the specimens.

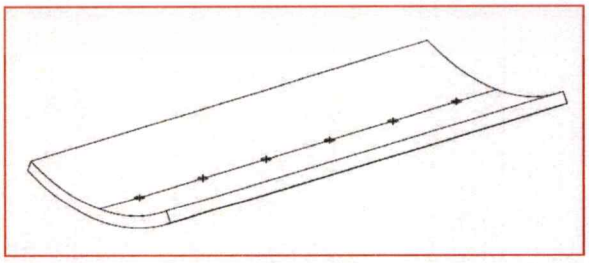

Figure 3.9 Measurement positions for hardness testing on liner specimen

From the obtained results in Table 3.5, the averaged surface hardness of liner specimens were about 24 HRC. As a result, ball steels of 58 HRC hardness as referred by the manufacturer were chosen for the micro-tribometer testing.

Table 3.5 Hardness measurement results of the liner specimens

Point	HRC Scale Load 1471 N	
	Specimen I	Specimen II
1	24.6	23.7
2	24.8	24.1
3	24.1	23.1
4	23.7	24.3
5	24	24.9
6	25	23.5
Average	24.3	23.9

Furthermore, the chemical compositions and the microstructure images of cylinder wall specimen are shown in Table 3.6, Figure 3.10 and Figure 3.11 respectively. The results were typical of a grey cast iron.

Table 3.6 Chemical compositions of cylinder wall

Element	C	Si	Mn	P	S	Cr	Cu
%	3.2668	2.4634	0.5322	0.2871	0.0330	0.1804	0.12637

Figure 3.10 Microstructure of cylinder wall specimen (500X)

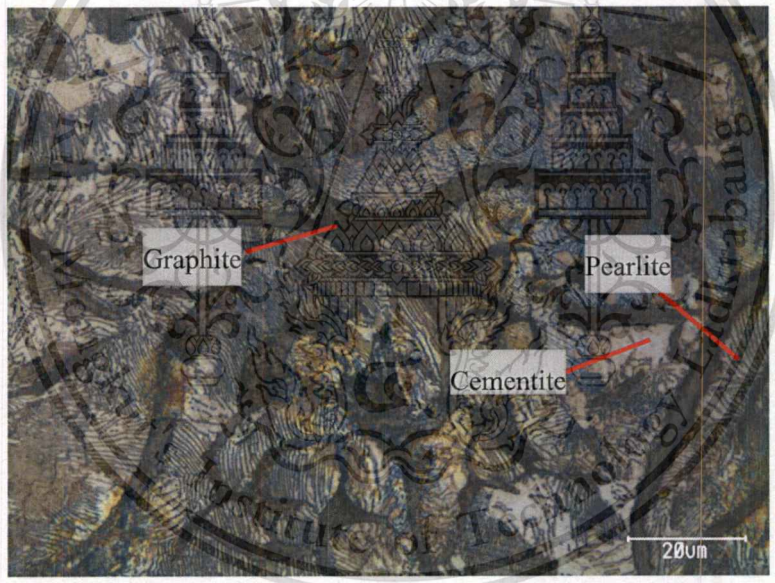

Figure 3.11 Microstructure of cylinder wall specimen (20X)

3.2.6 Experimental procedures

(1) Carry out an engine load test on two single cylinder diesel engines running with difference fuels in each engine i.e. diesel and biodiesel. Two tests were done separately for each engine i.e. test duration of 50 hours and 200 hours. The used lubricant oil was collected after each testing. At the beginning of each test, new

spare parts such as piston, piston rings, liner, bush bearing, and connecting rod bearing were replaced into the test engines.

(2) Examine the lubricant conditions by testing samples of fresh lubricant oil and used lubricant oils by a rotational rheometer for viscosity analysis test.

(3) Further examine the lubricant conditions by spectroscopy analysis using Fourier Transform Infrared spectroscopy (FTIR) and Inductively Couple Plasma Spectrometer (ICP) techniques for oil contamination analysis and for wear condition analysis respectively.

(4) Prepare an additional set of lubricant samples by adding a carbon black powder into a fresh lubricant oil by controlled %weight of 0.25%, 0.5%, 0.75%, 1%, 1.5%, 2%, 2.5%, 3%, 3.5%, and 4%. The maximum %weight was 4% because the mixture would become too thick. Then obtain the absorbance values of lubricant samples by Fourier Transform Infrared spectroscopy (FT-IR) to determine the percentage of soot contamination in tested lubricant oil by weight.

(5) Prepare another set of lubricant samples by mixing some biodiesel and biodiesel with fresh lubricant oil by %volume of 1%, 2%, 3%, 4%, 5%, 6%, 7%, 8%, 9%, 10%, 25%, and 50%. Then obtain the absorbance ranges of lubricant samples by Fourier Transform Infrared spectroscopy (FTIR) for determine the percentage of fuel contamination in tested lubricant oil by volume.

(6) Prepare the liner specimens by wire-cutting method. Then use them for wear simulation testing in Tribometer testing machine.

(7) Perform specimen wear scar inspection by a stylus roughness measurement machine.

(8) Result analysis and conclusions.

CHAPTER 4

RESULTS

4.1 Wear condition analysis by Inductively Couple Plasma Spectrometer (ICP)

As shown in Figure 4.1, the lubricant oils were collected from the engine reservoir after the engines were operated on each assigned condition explained in the previous chapter. The wear condition occurred in the engine during the test could be analyzed by means of performing an Inductively Couple Plasma Spectrometer (ICP) technique on the collected lubricants and the fresh lubricant according to USEPA 3052:1996 standards. Several inorganic elements which were related to engine parts and lubricant additives were chosen for detection. The obtained results are summarized in Table 4.1.

Figure 4.1 Lubricant oil samples for analytical tests

Table 4.1 Wear condition analysis by Inductively Couple Plasma Spectrometer (ICP)

Testing item content	Result of used oil (mg/kg)				
	$Lub._{fresh}$	$Lub._{Diesel\_50\ hr}$	$Lub._{Diesel\_200\ hr}$	$Lub._{B100\_50\ hr}$	$Lub._{B100\_200\ hr}$
Aluminum (Al)	ND	2	2	13	9
Chromium (Cr)	ND	ND	ND	ND	ND
Copper (Cu)	ND	ND	ND	ND	ND
Iron (Fe)	ND	20	39	18	62
Lead (Pb)	ND	ND	ND	ND	ND
Phosphorus (P)	324	188	124	288	165
Silicon (Si)	ND	ND	ND	ND	3
Nickel (Ni)	ND	ND	ND	ND	ND
Zinc (Zn)	76	189	42	159	65

Remark: mg/kg = Milligram per kilogram based on weight of sample = ppm

ND = Not Detected

Testing method = With reference to USEPA 3052:1996, by Acid digestion and determined by ICP-OES

Reporting limit = Quantitative limit analyze in sample

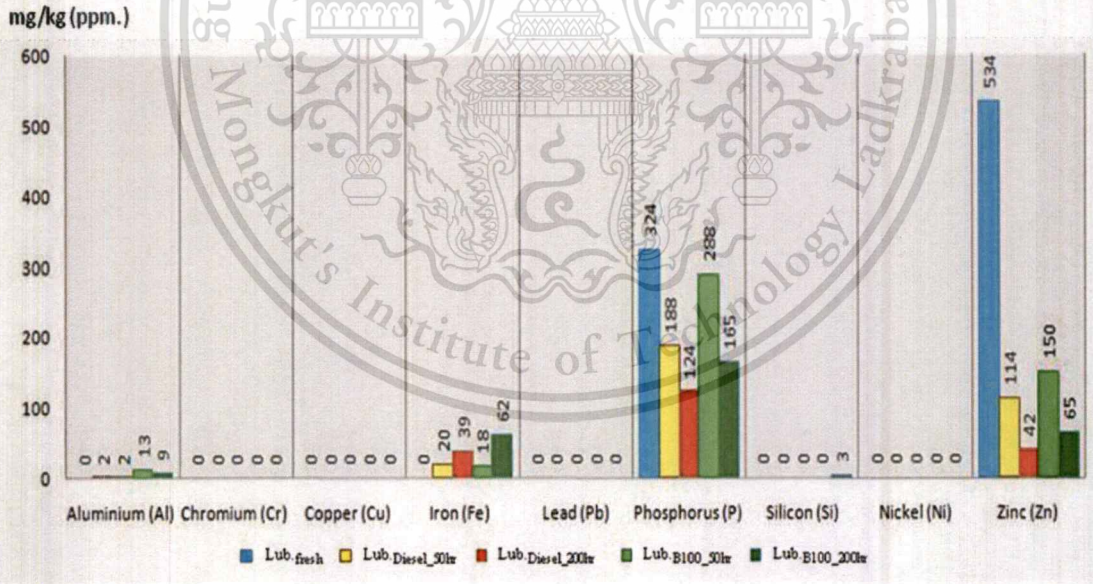

Figure 4.2 Wear condition results by Inductively Couple Plasma Spectrometer (ICP-OES)

The measured quantity of metals and residual additives from used lubricant oils are displayed graphically in Figure 4.2. The graphs showed higher detectable amounts of aluminum and Iron element from used lubricant oil of biodiesel-fueled engine than those of diesel-fueled

engine. As for phosphorus and zinc, they were major component of the anti-wear additive zinc dialkyldithiophosphates (ZDDP). The graphs of ICP showed higher detectable amounts of both elemental from used lubricant oil of biodiesel-fueled engine than diesel-fueled engine. The detection of aluminum element could be assumed that came from the wear of piston, connecting rod bearings, valves and connecting rod bushing. On the other hand, the presence of iron could be by the wear of metal parts such as liner, shafts, gear and bearing.

4.2 Lubricant oil condition analysis

In another part of lubricant oil condition analysis, a rotational Rheometer was employed to measure a dynamic viscosity of tested lubricant oils over a range of temperature as shown in Table 4.2 (20-150°C). The measured results are compared together and displayed graphically in Figure 4.3.

Table 4.2 Dynamic viscosity of lubricant oil at several temperatures

Lubricant oil	Viscosity, η (Pas)				
	20°C	60° C	85° C	100° C	150°C
$Lub._{fresh}$	0.4866	0.06254	0.01885	0.00997	0.006034
$Lub._{Diesel\_50hr}$	0.4907	0.06752	0.02232	0.01398	0.01062
$Lub._{Diesel\_200hr}$	1.862	0.3151	0.2479	0.2503	0.3714
$Lub._{B100\_50hr}$	0.4419	0.06066	0.0216	0.01364	0.009776
$Lub._{B100\_200hr}$	0.6268	0.07657	0.02852	0.01585	0.01628

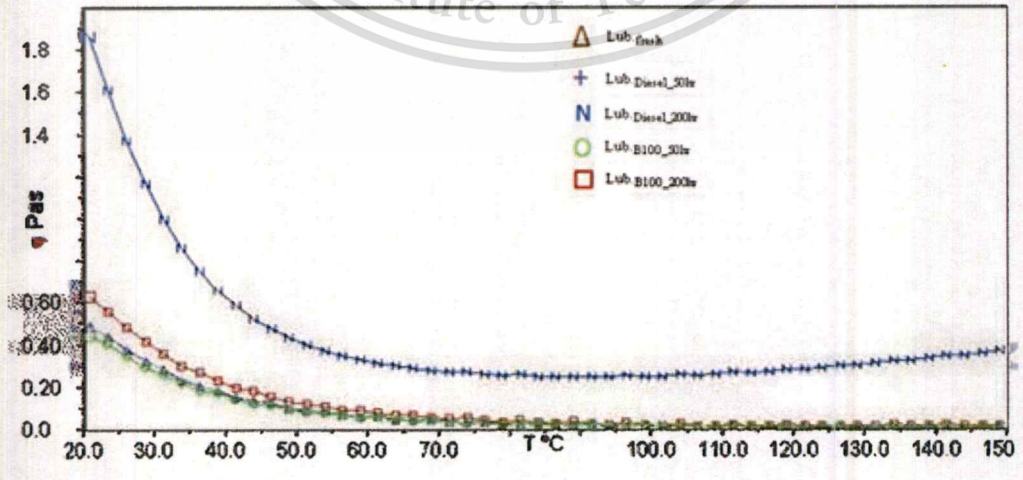

Figure 4.3 Dynamic viscosity comparison of the tested lubricant oil samples

The curve in Figure 4.3 showed the comparison of viscosity of lubricant oil samples from both engines running on different fuels with the fresh lubricant oil. For all samples, the dynamic viscosity decreased at a reducing rate as the temperature went up. More importantly, It could be seen that that the deviations of lubricant oil sample from both engines after 200 hours were relatively high especially with the lubricant oil from diesel-fueled engine.

4.3 Lubricant oil contamination analysis

As explained in previous chapter, the Fourier Transform Infrared Spectroscopy testing (FT-IR) would illustrate a picture of lubricant oil's health and also whether any contaminants were presented such as fuel or coolant. In this study, the purpose of this test was to investigate how the lubricant oil condition changed from its virgin state to its used state by comparing the frequency spectrum of used lubricant oil to that of the fresh lubricant oil. A typical frequency spectrum is displayed in Figure 4.4. The standard of testing was referred from ASTM E2412-04 as shown in Table 4.3.

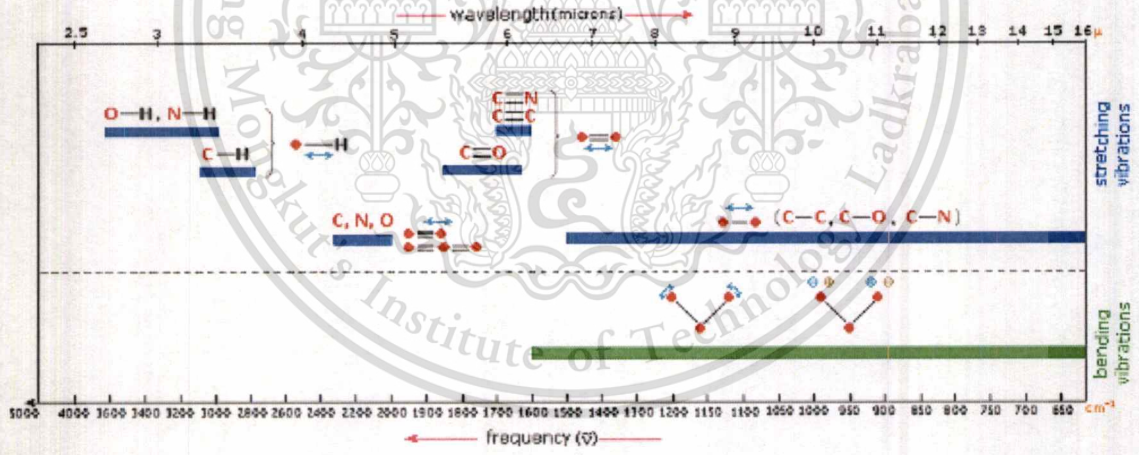

Figure 4.4 The frequency spectrum standard

Table 4.3 The standard of testing from ASTM E2412-04

Component	Measurement Area, cm^{-1}	Baseline Point(s), cm^{-1}	Reporting
Water	Area 3500 to 3150	Minima 4000 to 3680 and 2200 to 1900	Value as Measured
Soot Loading	Absorbance intensity at 2000	None	Value x 100
Oxidation	Area 1800 to 1670	Minima 2200 to 1900 and 650 to 550	Value as Measured
Nitration	Area 1650 to 1600	Minima 2200 to 1900 and 650 to 550	Value as Measured
Antiwear Components (Phosphate based, typically ZDDP)	Area 1025 to 960	Minima 2200 to 1900 and 650 to 550	Value as Measured
Diesel	Area 815 to 805	Minima 835 to 825 and 805 to 795	(Value+2) x 100
Sulfate by-products	Area 1180 to 1120	Minima 2200 to 1900 and 650 to 550	Value as Measured
Ethylene Glycol Coolant	Area 1100 to 1030	Minima 1130 to 1100 and 1030 to 1010	Value as Measured
Instrument :	FT-IR Spectrometer (Perkin Elmer System 2000R)		
Test method :	FT-IR technique		
Conditions :	Light source: Middle range infrared (4000-400 cm^{-1})		
Resolution :	4 cm^{-1}		
Scan :	16		
Detector :	TGS		

The FT-IR results in Table 4.4 showed that lubricant oils from biodiesel-fueled engine after running for 50 and 200 hours had higher level of water, oxidation, nitration, anti-wear components, sulfate and ethylene glycol coolant than the lubricant oil from diesel-fueled engine.

Only a soot loading from lubricant oil of diesel-fueled engine was higher than the lubricant oil of biodiesel-fueled engine.

Table 4.4 FT-IR report (unit: absorbance/0.1 mm)

Component	$Lub._{fresh}$	$Lub._{B100\_50hr}$	$Lub._{Diesel\_50hr}$	$Lub._{B100\_200hr}$	$Lub._{Diesel\_200hr}$
Water	2.0803	4.7507	3.504	5.904	5.7767
Soot Loading	0.63	5.21	15.81	67.72	92.38
Oxidation	0.8519	2.4289	0.8276	4.5367	2.1754
Nitration	1.0399	1.7882	1.513	3.4176	2.5215
Anti-wear Components*	3.2145	4.165	3.2875	4.9615	4.318
Sulfate by-products	2.5047	4.3107	3.4075	7.3575	5.7357
Ethylene Glycol Coolant	0.1781	0.1891	0.1004	0.1372	0.0524
Remark * =Phosphate based, typically ZDDP					

A bar chart could be created from the data in Table 4.4 as shown in Figure 4.6 for a comparison of lubricant contaminations between both fuels. Figure 4.5 shows a relative amount of soot on the pistons disassembled from each engine test. A higher amount of soot deposition could be clearly seen on the pistons taken from 200-hours tests for both type of fuels.

Figure 4.5 Soot deposition on the piston disassembled from the test engines.

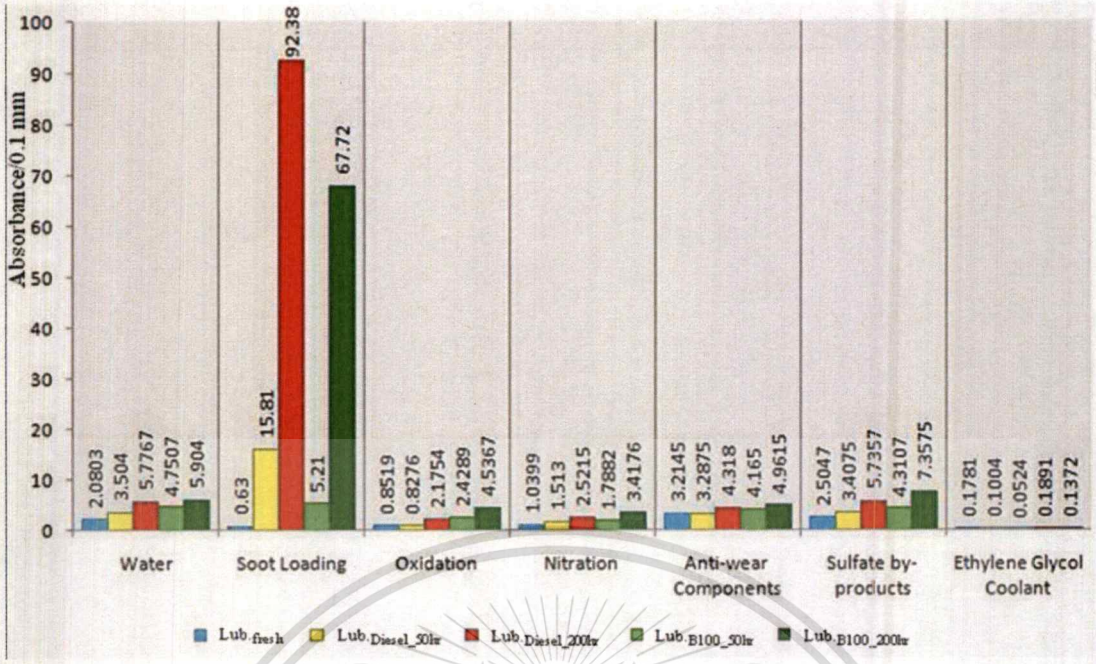

Figure 4.6 FT-IR result of lubricant oil contamination

From Figure 4.6, seven different contaminations were considered in the FT-IR results, namely; water, soot loading, oxidation, nitration, anti-wear components, sulfate by-products and ethylene glycol coolant. The impact of each contamination on the engine could be explained as followed:

- Water contamination indicates the degradation of lubricant oil because this contamination could reduce the lubricity of lubricant oil. The presence of water alone does not necessarily indicate a coolant problem, but may be a result from condensation due to a low operating temperature or oxidation from fuel contamination. The obtained FT-IR results indicated the used lubricant oil from biodiesel-fueled engine had slightly higher water contamination than diesel-fueled engine.
- Soot loading indicates the engine has incomplete combustion of fuel or clogged air filter or an exceeded lubricant oil change period. From the obtained FT-IR results, used lubricant oil of diesel-fueled engine had higher soot contamination than biodiesel-fueled engine. During the 50-hours and 200-hours test, diesel-fueled engine has higher soot contamination more than that of biodiesel one by about 3 times and 1.4 times respectively. Comparing between the 50-hour and 200-hour results, the proportion of

increase in soot contamination in lubricant oil from biodiesel-fueled engine was higher than 13 times in contrast to that of diesel-fueled engine with an increase of 6 times. Overall, the soot contaminations of all used lubricant oils were higher than fresh oil significantly.

- Oxidation value can indicate lubricant oil degradation by either workload, time of using, or operating temperature. This could mean an increase in viscosity of the lubricant oil. From the experimental results, the analysis showed that the oxidation value from used lubricant oil samples was rising with the test duration. Furthermore the lubricant oil from biodiesel-fueled engine had higher oxidation value than the lubricant oil from diesel-fueled engine in both 50- and 200-hour of running engine by about 2-3 times.
- Nitration value is related to nitrogen oxides produced from the oxidation of atmospheric nitrogen during the combustion process reacting with the lubricant oil. Nitration could increase the viscosity of the lubricant oil and is the major cause of the build-up of varnish or lacquer. The results showed that the lubricant oil from biodiesel-fueled engine had nitration value closed to the lubricant oil from diesel-fueled engine in 50-hours of engine test and slightly higher in 200-hours testing.
- Anti-wear components (Phosphate based, typically ZDDP). The most commonly used anti-wear additives are zinc di-alkyl or di-aryl dithiophosfates (ZDDP's). These additives are consumed during the normal life of the lubricant oil. Consumption of anti-wear additive is accelerated by the presence of water. A rapid loss of anti-wear additive may indicate excess loads or contamination by water from a coolant leak. This value can prove quantity of residual additives in used lubricant oil. The results showed that the quantity of residual additives in used lubricant oil from biodiesel-fueled engine was higher than that in used lubricant oil from diesel-fueled engine. This was the same trend as observed in ICP results.
- Sulfate by-products value could be a result of the combustion of sulfur compounds in oil and fuel from which the chemical reaction produces some product such as dirt, gum deposited at the piston and rings. The results showed the lubricant oil from biodiesel-fueled engine had higher sulfate value than the lubricant oil from diesel-fueled engine in both 50- and 200-hours of engine test.

- Ethylene Glycol Coolant is the presence of water and glycol and could indicate a leak from the cooling system. It could lead to lubricant oil degradation, slugging, wear, and corrosion. The result showed that the used lubricant oil from both fueled engines had very little contamination of this type.

In addition to contaminations explained above, another important lubricant contamination is a fuel contamination. The FT-IR result could be used to show the leakage of fuel through the piston rings into the crankcase. The fuel contamination could lead to lubricant dilution which could change main lubricant properties such as viscosity, chemical, and pHs values. These changes could have a major impact on the performance of the lubricant to prevent wear. As a result, the information about the amount of fuel contamination in oil samples collected from the engines was important.

However, since the values obtained from the FT-IR, as shown in Table 4.4 or Figure 4.6, was an absorbance of organic elemental functional group. A calibration method was needed in order to determine the percentage of fuel contamination by volume. Similarly, the same approach was also used to determine the percentage by weight of soot contamination in the collected lubricants. Thus, an additional experiment was introduced such that a batch of fresh lubricant was mixed separately with either diesel or biodiesel or carbon black power at controlled ratios. Then, FT-IR analysis was performed on the mixtures to determine the corresponding absorbance spectrums. The obtained range of FT-IR spectrum data was used to evaluate the trend line and the corresponding equation of relationship between absorbance and the known percentage of contaminant. This corresponding equation could then be used to estimate the percentage of diesel or biodiesel or soot contamination in collected lubricant oil samples. The measurement area graph of the FT-IR wavenumbers for this particular test is shown in Table 4.5.

Table 4.5 FT-IR calibrated method

Component	Measurement Area, cm^{-1}	Baseline Point(s), cm^{-1}	Reporting Units
Soot	Height at 1950	No baseline	A/cm or wt%
Diesel	Area 817 to 804	2 point 817 and 804	wt%
Ester	Area 1390 to 1090	2 point 1390 and 1090	volume%
C=O	Area 1800 to 1700	2 point 1800 and 1700	volume%

The used lubricant oil sample was a complex mixture of a large number of different compounds derived from the original fresh lubricant oil, its additives, lubricant oil degradation products and contaminants. The resulting FT-IR spectrum was essentially the sum of the spectra of all of its components and consisted of a large number of overlapping peaks as shown in Figure 4.7.

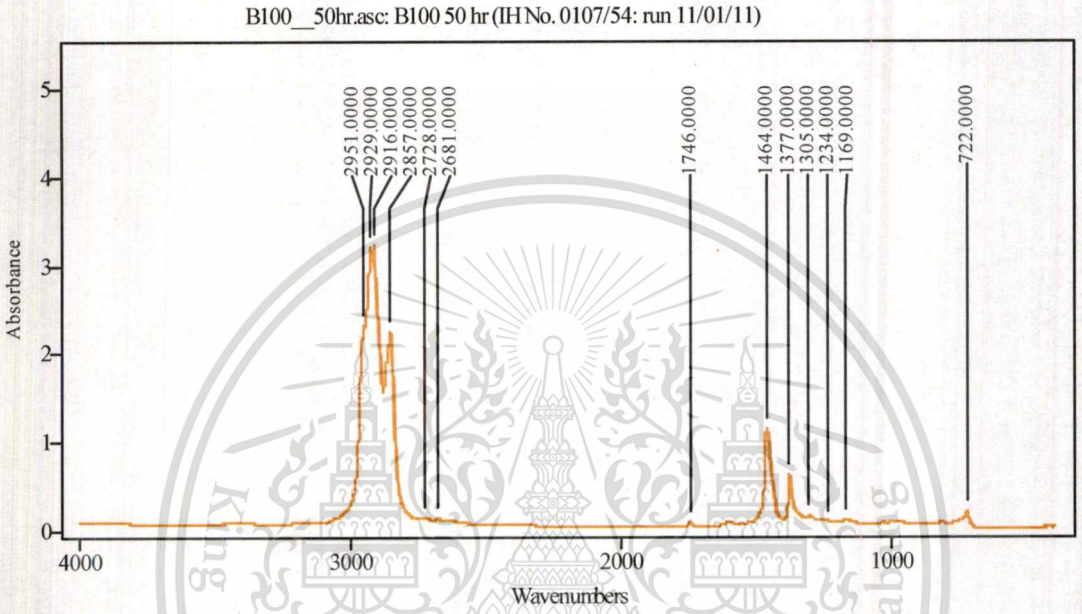

Figure 4.7 Example of FT-IR spectrum of used lubricant oil sample

Since the main concern about the used lubricant analysis was about the changes that had occurred during the engine test, spectrums of pure biodiesel, diesel, and fresh lubricant oil were needed as a reference as shown in Figure 4.8 to Figure 4.11.

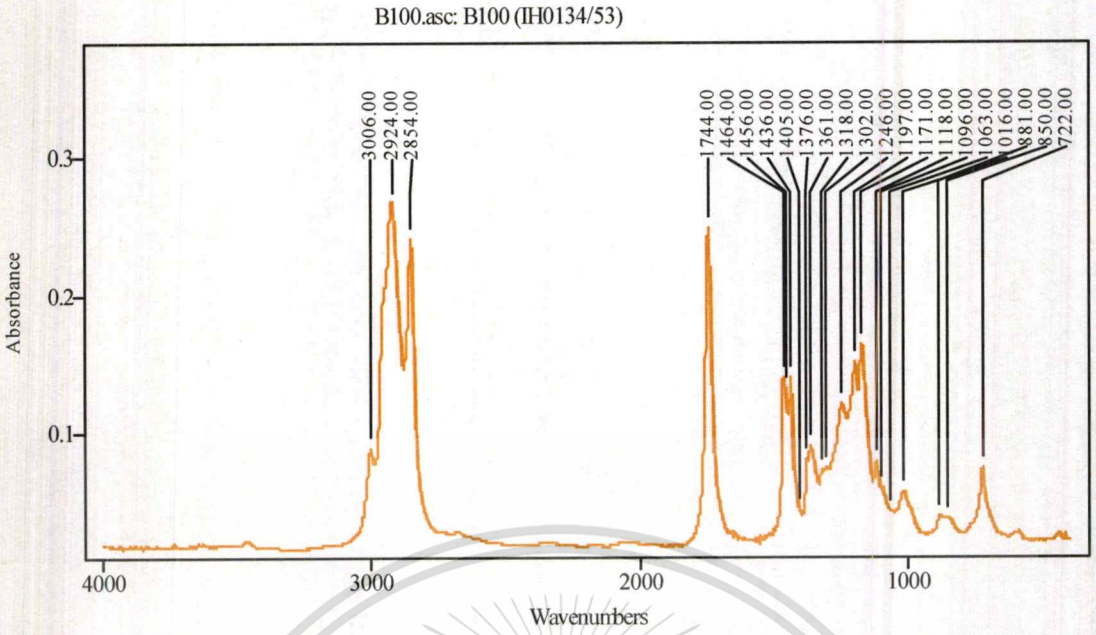

Figure 4.8 The infrared spectrum of biodiesel sample

The infrared spectrum of biodiesel is shown in Figure 4.8. The strong ester peaks at 1744 cm^{-1} (the C=O vibration) and around 1170-1200 cm^{-1} (C-O vibrations) could be clearly identified.

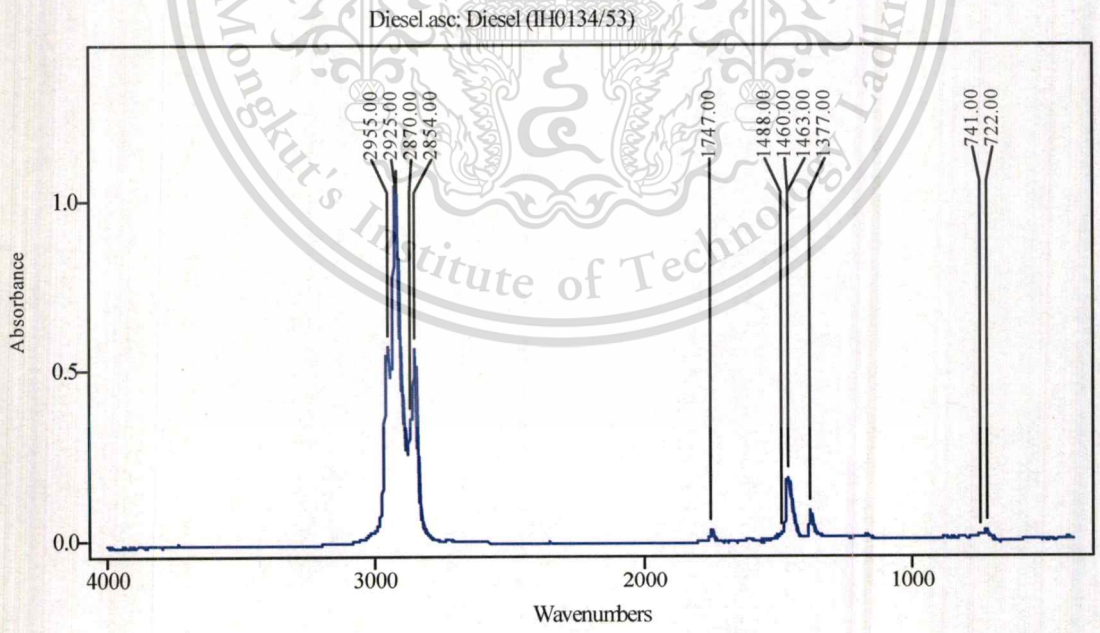

Figure 4.9 The infrared spectrum of Diesel (Biodiesel 3%)

The infrared spectrum of Diesel (Biodiesel 3%) is shown in Figure 4.9. The weak ester peaks at 1747 cm^{-1} (the C=O vibration) and around 1170-1200 cm^{-1} (C-O vibrations) could be seen.

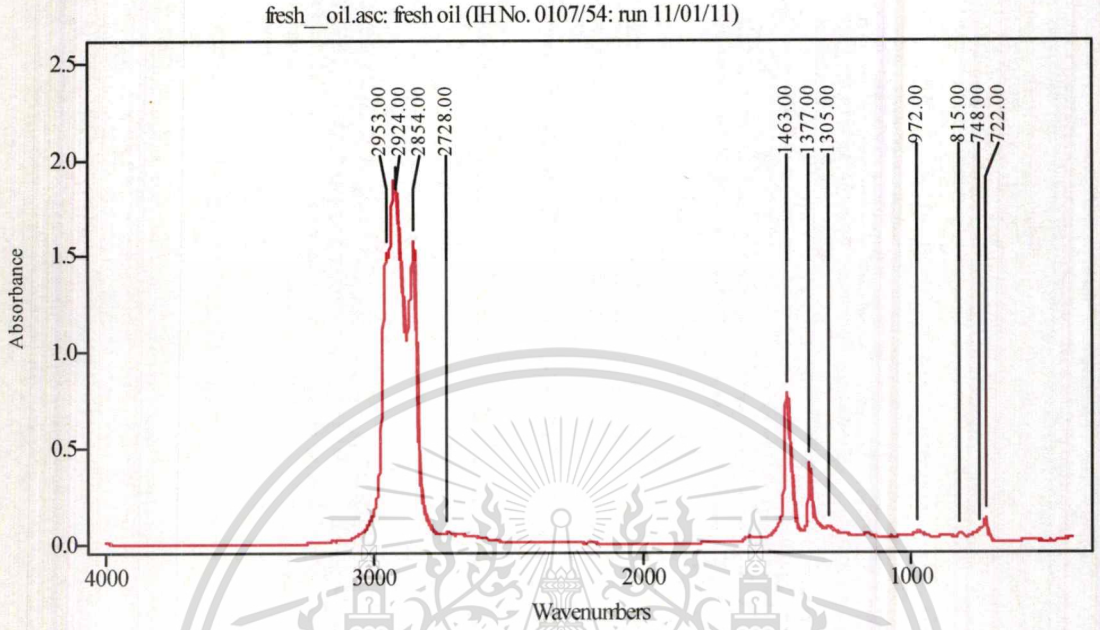

Figure 4.10 Infrared spectrum of fresh oil

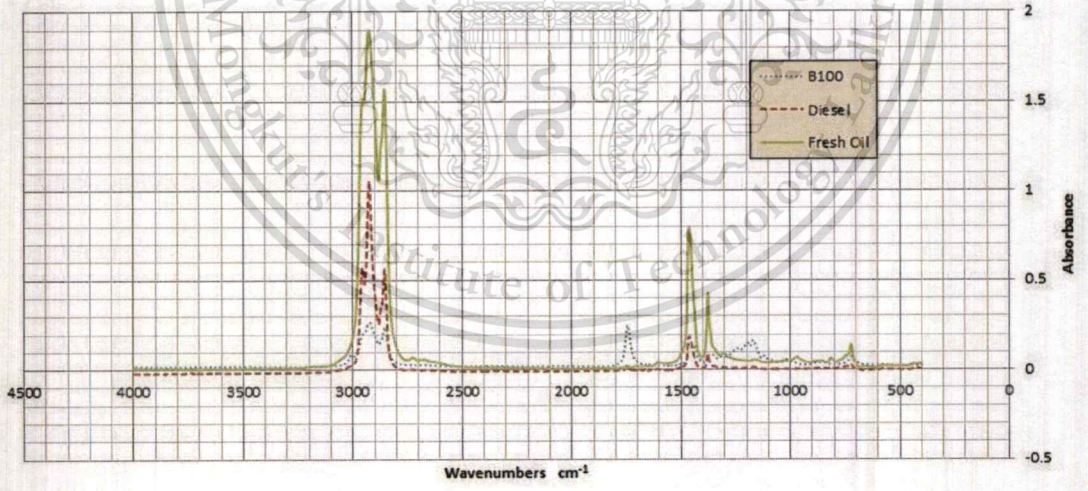

Figure 4.11 Infrared overlay spectrum of biodiesel, diesel and fresh oil

As mentioned earlier, in order to find percentage of diesel contamination in lubricant oil by volume, the calibration method involving FT-IR on diesel-mixed lubricant was carried out. The diesel was blended at the ratio of 1%, 2%, 3%, 4%, 5%, 6%, 7%, 8%, 9%, 10%, 25% and 50% by

volume and the mixtures were analyzed for their absorbance values. The measured absorbances were then plotted against their respective blend ratio to allow the correlating equation between the two parameters to be determined as shown in Figure 4.12. The obtained equation of a linear relationship was used to calculate the proportion of a fuel leak over into the crankcase from each engine test as shown in Table 4.6.

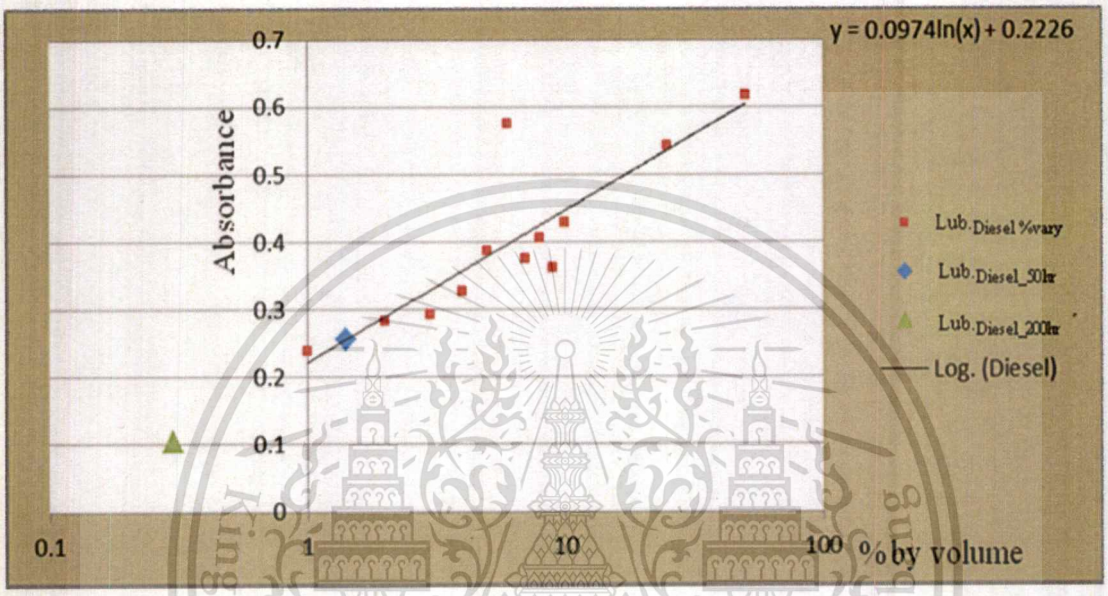

Figure 4.12 Diesel contamination in lubricant oil by volume and the equation of a linear relationship

Table 4.6 Estimated diesel contamination in tested lubricant oils by volume

Lubricant of Diesel engine	Absorbance	Diesel volume%
50hr	0.2558	1.40942
200hr	0.105	0.301955

From the results, the diesel contamination percentage of the used lubricant oil sample of diesel-fueled engine from 200-hours test was less than that of 50-hours test. The lower contamination percentage in 200-hours lubricant was assumed to be due to the unburned fuel creeping down to the crankcase being evaporated through leakages of the engine. This was because typically the diesel fuel had a flash point of approximately 60 °C while temperature in the crankcase was approximately 80 °C.

Similarly, in order to determine the percentage of soot contamination in the collected lubricants, a commercial carbon black powder was mixed with the fresh lubricant oil in the mixing ratio 0.75%, 0.25%, 0.5%, 1.5%, 1%, 2%, 3%, 2.5%, 3.5% and 4% by weight. The measured absorbances from FT-IR were then plotted against their respective blend ratio to allow the correlating equation between the two parameters to be determined as shown in Figure 4.13. The obtained equation of a linear relationship was used to calculate the proportion of soot contamination from each engine test as shown in Table 4.7.

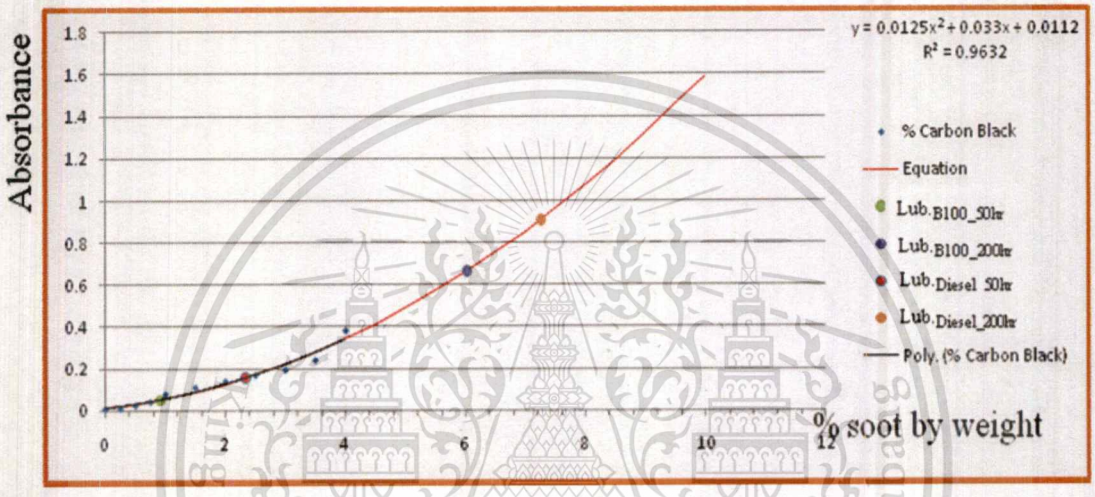

Figure 4.13 The percentage of soot contamination by weight and the curve-fitting equation

Table 4.7 Estimated percentage by weight of soot contamination

Lubricant	Absorbance	Soot weight%
B100@50hr	0.050694	0.904177
B100@200hr	0.663506	6.022865
Diesel@50hr	0.156292	2.334073
Diesel@200hr	0.909889	7.262294

The percentage by weight of soot shown in Table 4.7 suggested that the soot contamination of used lubricant oil from diesel-fueled engine was higher from both 50- and 200- hours tests. The results corresponded to the measured viscosity by the Rheometer reported earlier. The increase of soot was a main cause of the increases in lubricant viscosity.

Furthermore, for the contamination of biodiesel in the used lubricant oil sample, a range of FT-IR absorbance from the functional group of biodiesel chemical formula, i.e. the ester and carbonyl (C = O), were used to analyze the amount of contamination. A basic reaction of biodiesel production has a chemical formula as shown in Figure 4.14.

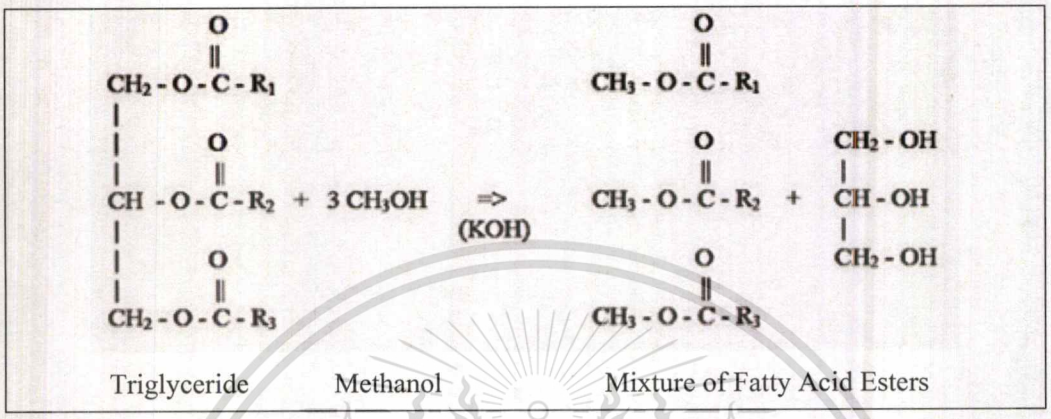

Figure 4.14 Basic chemical reaction of biodiesel fuel production

In a sample preparation, a biodiesel was blended into the fresh lubricant at the controlled ratio of 1%, 2%, 3%, 4%, 5%, 6%, 7%, 8%, 9%, 10%, 25% and 50% by volume. The carbonyl (C = O) peak was investigated first. The measured absorbances were then plotted against their respective blend ratio to allow the correlating equation between the two parameters to be determined as shown in Figure 4.15.

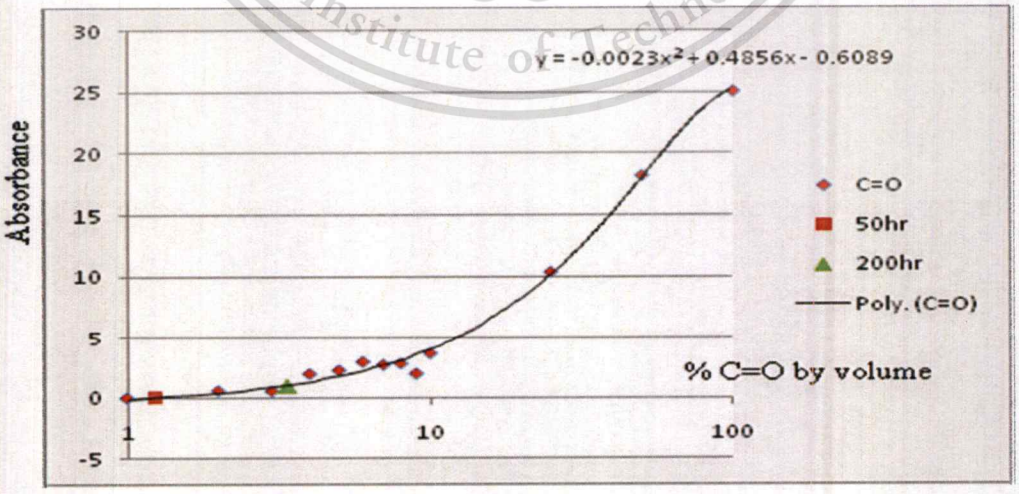

Figure 4.15 The percentage by volume of carbonyl (C = O) contamination and the correlating equation

The obtained polynomial correlating equation was used to calculate the proportion of a biodiesel fuel leak over into the crankcase from each engine test as shown in Table 4.8.

Table 4.8 Estimated percentage by volume of carbonyl (C = O) contamination

Biodiesel	Absorbance	C=O volume%
B100@50hr	-0.01577	1.228591
B100@200hr	0.993348	3.352764

Additionally, the same FT-IR results of lubricant collected from engine tested with biodiesel were further analyzed for ester peak. The measured absorbance values were then plotted against their respective blend ratio to allow the correlating equation between the two parameters to be determined as shown in Figure 4.16. The obtained polynomial correlating equation was used to calculate the proportion of a biodiesel fuel leak over into the crankcase from each engine test as shown in Table 4.9.

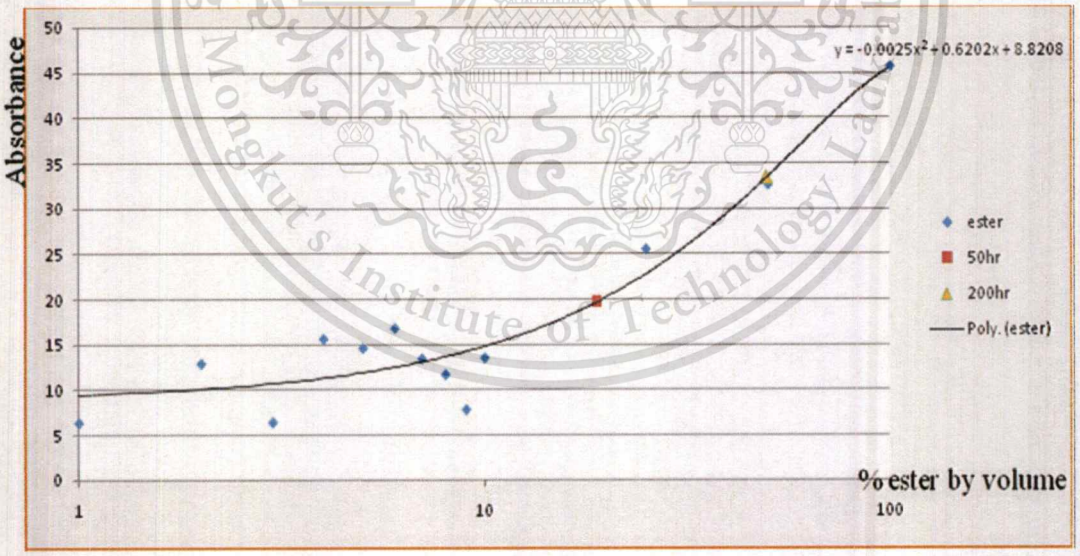

Figure 4.16 The percentage by volume of ester contamination and the correlating equation

Table 4.9 Estimated percentage by volume of ester contamination

Biodiesel	Absorbance	Ester volume%
B100@50hr	19.68649869	18.97029874
B100@200hr	33.42134933	49.57053063

The estimated values of carbonyl and ester contamination from the both periods of engine tests showed that the level of contamination had increased over the period of engine operation. In this study, the ester volume was chosen as the representative of biodiesel contamination since the carbonyl group was a subset of the ester. Therefore, it could be concluded that the 50-hours lubricant had a contamination of the ester about 19 percent by volume while the 200-hours lubricant had a contamination of the ester about 49.5 percent by volume.

Moreover, the corresponding dynamic viscosities of the mixed blends from the FT-IR calibration tests were measured as shown in Figure 4.17. This was for determining the parameters of tribometer testing as will be explained in the next section.

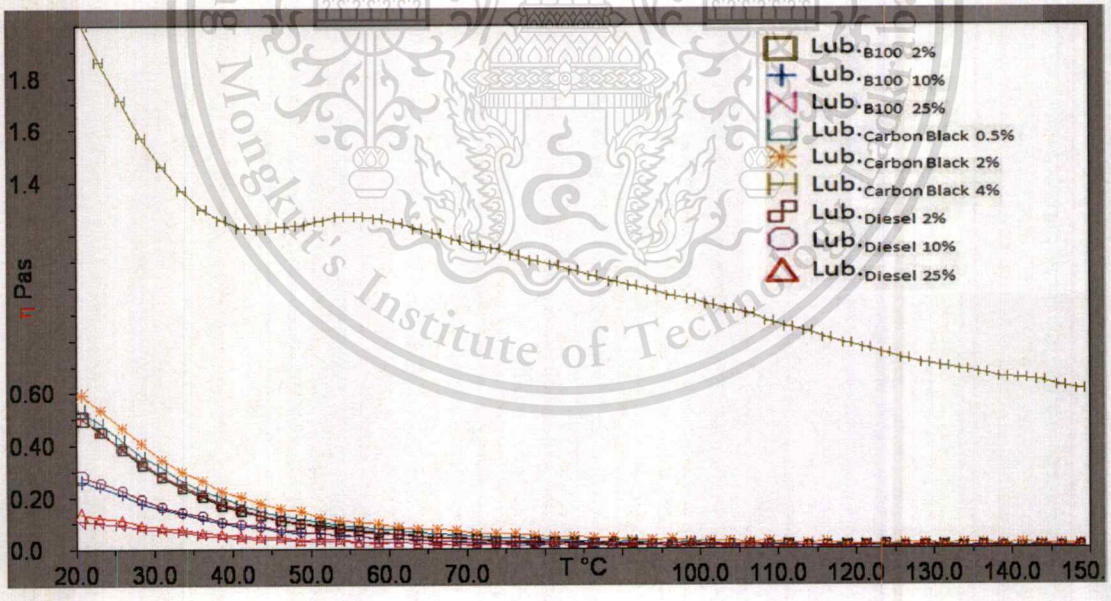

Figure 4.17 Dynamic viscosity of blended lubricant oil samples from FT-IR calibration test

4.4 Reciprocating wear simulation by Micro-Tribometer Testing

The wear performance of the lubricant oil samples collected from diesel and biodiesel-fueled operating engines was qualitatively investigated by means of an abrasion test with Micro-Tribometer shown in Figure 4.18. As explained in previous chapter, the test specimens were prepared from the cylinder wall (Liner) as shown in Figure 4.19. Also the counterface parts which were a ball steel had been chosen to have a higher surface hardness than that of the specimens to concentrate the occurrence of wear on the specimens. The tests were performed on the center track of the specimen with sliding direction along the axial direction of the specimen i.e. in the same direction as of the piston moving in the engine.

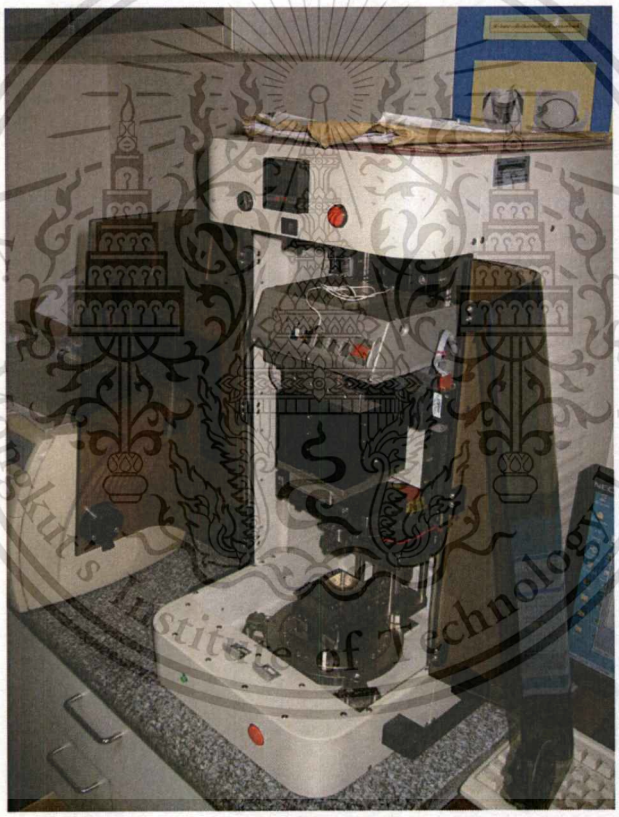

Figure 4.18 Micro-Tribometer UMT-2 (Universal Material Tester)

At the beginning of each test, the reciprocating stage was cleaned by solvents. Then, the new liner specimen and the ball steel were installed onto the tribometer. The heater used for controlling the test temperature was set within a range of about 80 ° C. This was to simulate the temperature inside the engine as closed as possible.

Figure 4.19 Example of wire-cut liner specimens for tribometer test

After the test, the specimen was taken out and cleaned with solvent in an ultrasonic bath. The resulting depth of abrasion was measured with the roughness profiler machine. The measurement direction was in a transverse direction to the abrasion scar or along the perimeter of the inside diameter of the specimen as shown in Figure 4.20. Then, the depth of the abrasion could be estimated from the obtained surface profile shown in Figure 4.21.

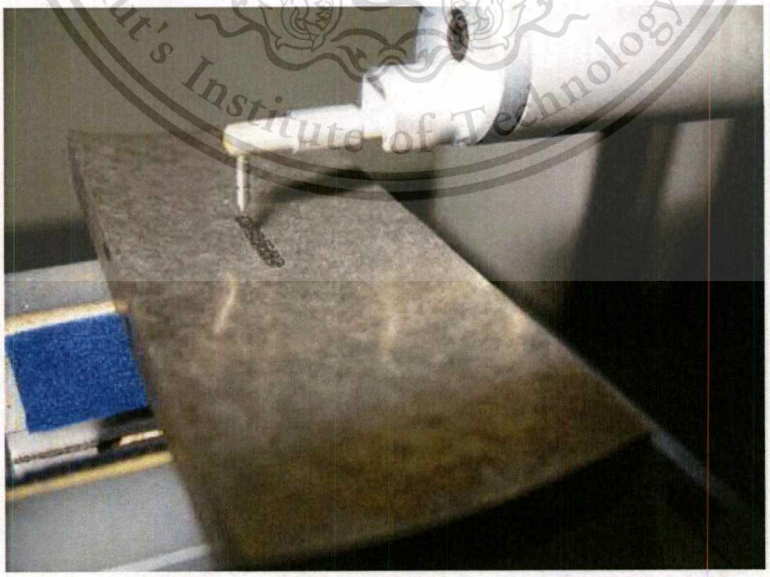

Figure 4.20 Surface roughness measurement procedure

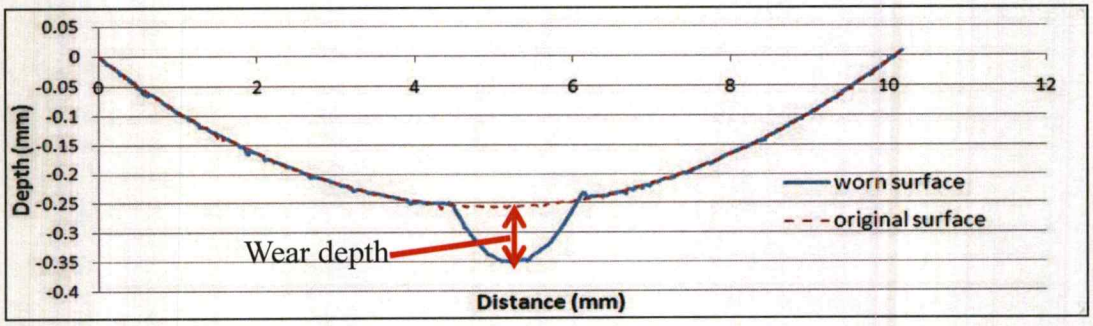

Figure 4.21 Estimated depth of the abrasion

All the measurements were done three times after the test. The tribometer test results are shown in Table 4.10. Generally, the specimens from used lubricant oil of diesel-fueled engine showed a higher averaged depth of abrasion scar and weight loss than those from the used lubricant oils of biodiesel-fueled engine as presented graphically in Figure 4.22.

Table 4.10 Tribometer Results: abrasion depth and weight lost measurements

Lubricant	No.	Wear depth (mm)	Wear depth average (mm)	Weight lost (g)	Weight lost average (g)
$Lub._{fresh}$	1	0.011437	0.021170667	0.0032	0.00546
	2	0.006862		0.0058	
	3	0.045213		0.0074	
$Lub._{Diesel\_50hr}$	1	0.058325	0.041796	0.0089	0.00633
	2	0.056463		0.0064	
	3	0.0106		0.0037	
$Lub._{B100\_50hr}$	1	0.049188	0.029550333	0.0103	0.00793
	2	0.006925		0.0075	
	3	0.032538		0.006	
$Lub._{Diesel\_200hr}$	1	0.088649	0.113266667	0.0097	0.01206
	2	0.131013		0.0143	
	3	0.120138		0.0122	
$Lub._{B100\_200hr}$	1	0.089112	0.096924667	0.0082	0.00943
	2	0.110763		0.0095	
	3	0.090899		0.0106	

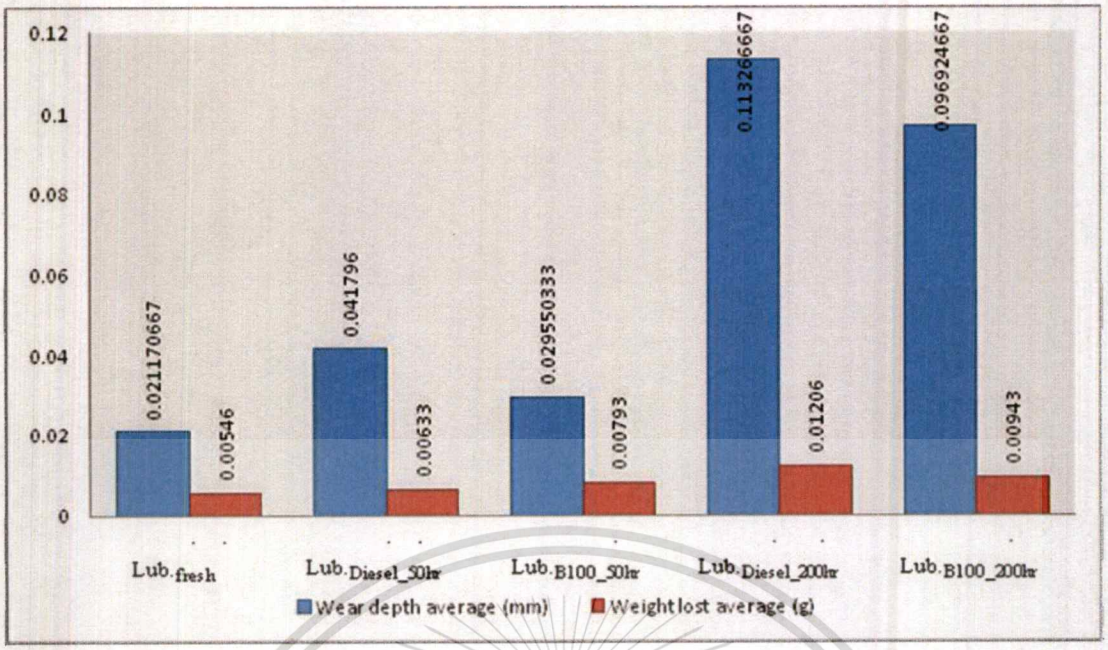

Figure 4.22 Tribometer results comparison

Furthermore, the batch of lubricant blends from FT-IR calibration experiment described in the previous section was also tested with the tribometer. In order to study the wear performance of different blends, the corresponding film thickness was chosen as a controlled parameter. As a result, an Elastohydrodynamic (EHL) film thickness calculation according to the tribometer contact geometry had to be carried out to find appropriated test conditions for each lubricant blend.

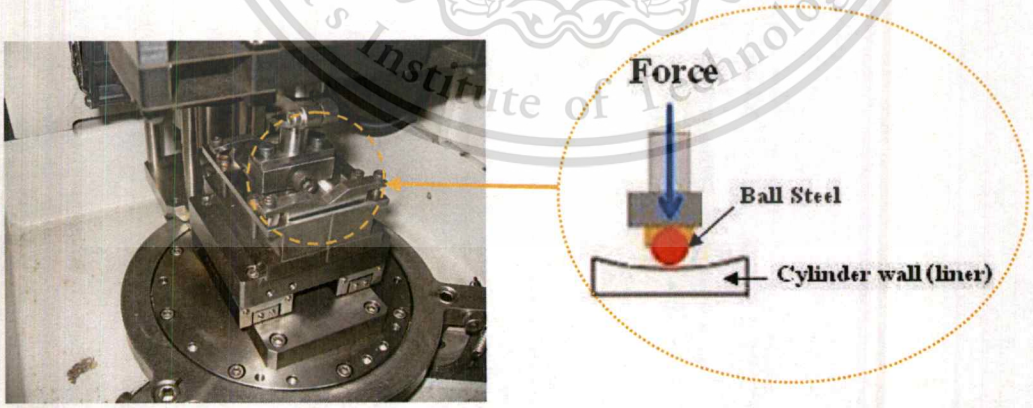

Figure 4.23 The contact geometry between ball steel and a cylinder wall (liner)

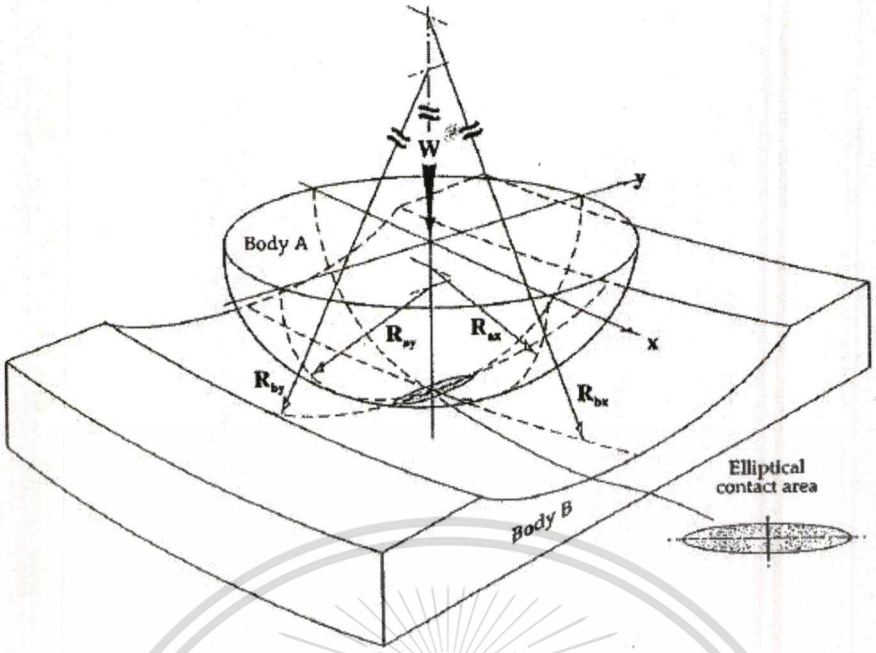

Figure 4.24 Schematic geometry of elliptical contact [19]

The contact geometry between a convex (ball steel) and a concave surface (liner) is displayed in Figure 4.23. From Figure 4.24, a body "B" has a concave surface and according to the theory its curvature is negative. The reduced radius (R') of curvature for this contact could be calculated according to equation (1):

$$\frac{1}{R'} = \left(\frac{1}{R_{ax}} + \frac{1}{R_{ay}}\right) - \left(\frac{1}{R_{bx}} + \frac{1}{R_{by}}\right) \tag{1}$$

Where: $\frac{1}{R_x} = \frac{1}{R_{ax}} - \frac{1}{R_{bx}}$ and $\frac{1}{R_y} = \frac{1}{R_{ay}} - \frac{1}{R_{by}}$

The evaluation of contact parameters is essential in many practical engineering applications. The most frequently used contact parameters are:

- The contact area dimensions
- The maximum contact pressure
- The average contact pressure

The contact area depends on the geometry of the contacting bodies, load and material properties. In most cases, the contact area is enveloped by an ellipse such as in the case of two cylinders crossed at an angle ≠90°. A circular contact area is found between two balls in contact or when two cylinders are crossed at 90°. The contact area between two parallel cylinders is enclosed by a narrow rectangle. The reduced Young's modulus (E') is defined as (2):

$$\frac{1}{E'} = \frac{1}{2}\left[\frac{1-\upsilon_A{}^2}{E_A} + \frac{1-\upsilon_B{}^2}{E_B}\right] \tag{2}$$

Where:

υ_A and υ_B are the Poisson's ratios of the contacting bodies A and B respectively;

E_A and E_B are the Young's modulus of contacting bodies A and B respectively.

Approximate formulae for contact parameters between two elastic bodies

- Contact area dimensions formulae for ellipse shape:

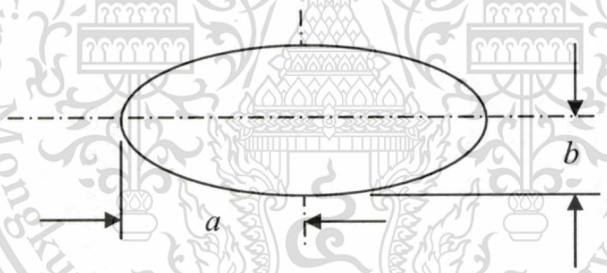

Figure 4.25 Contact area dimensions formulae for ellipse shape

$$a = \left(\frac{6\bar{k}^2\bar{\varepsilon}WR'}{\pi E'}\right)^{1/3} \tag{3}$$

$$b = \left(\frac{6\bar{\varepsilon}WR'}{\pi\bar{k}E'}\right)^{1/3} \tag{4}$$

- Maximum contact pressure:

$$P_{\max} = \frac{3W}{2\pi ab} \tag{5}$$

- Average contact pressure:

$$P_{average} = \frac{W}{\pi ab} \tag{6}$$

- Simplified elliptical integrals:

$$\bar{\varepsilon} = 1.0003 + \frac{0.5968 R_x}{R_y} \tag{7}$$

- Elliptic parameter:

$$\bar{k} = 1.0339 \left(\frac{R_y}{R_x} \right)^{0.636} \tag{8}$$

Where:

a	is the semimajor axis of the contact ellipse [m]
b	is the semiminor axis of the contact ellipse [m]
W	is the normal load [N]
$\bar{\varepsilon}$	are the simplified elliptic integrals;
$\bar{k}$	is the simplified elliptic parameter. The exact value of the elliptic parameter is defined as the ratio of the semi-axis of the contact ellipse in the transverse direction to the semi-axis in direction of motion.

The results of this analysis are the formulae for the calculation of the minimum film thickness in elastohydrodynamic contacts. The formulae derived by Hamrock and Dowson apply to any contact, such as point, linear or elliptical, and are now routinely used in EHL film thickness calculations including steel on steel even up to maximum pressures of 3-4 [GPa]. The numerically derived formulae for the minimum film thickness are in following form (9).

$$\frac{h_0}{R'} = 3.63 \left(\frac{U \eta_0}{E' R'} \right)^{0.68} \left(\alpha E' \right)^{0.49} \left(\frac{W}{E' R'^2} \right)^{-0.073} \left(1 - e^{-0.68k} \right) \tag{9}$$

Where:

h_0 is the minimum film thickness [m]

U is the entraining surface velocity [m/s],

i.e. $U = (U_A + U_B)/2$, where the subscripts A and B refer to the velocities of bodies A and B respectively;

η_0 is the viscosity at atmospheric pressure of the lubricant [Pas];

E' is the reduced Young's modulus [Pa];

R' is the reduced radius of curvature [m];

α is the pressure-viscosity coefficient [m^2/N];

W is the normal load [N]

k is the elliptic parameter defined as: $k = a/b$, where a is the semi-axis of the contact ellipse in the transverse direction [m] and b is the semi-axis in the direction of motion [m].

The pressure-viscosity coefficient (α) is a function of the molecular structure of the lubricant and its physical characteristics such as molecular interlocking, molecular packing and rigidity and viscosity-temperature characteristics. There are various formulae available to calculate the pressure-viscosity coefficient:

$$\alpha = (0.6 + 0.965 \log_{10}\eta_0) \times 10^{-8} \quad (10)$$

Where:

α is the pressure-viscosity coefficient [m^2/N];

η_0 is the atmospheric viscosity [cP], i.e. 1[cP] = 10^{-3} [Pas].

Table 4.11 The calculated results of normal force and maximum contact pressure

Normal Force (N)	a	b	Pmax [Mpa]
10	7.90144E-05	7.32027E-05	825.9018061
20	9.95518E-05	9.22296E-05	1040.571071
30	0.000113958	0.000105577	1191.156525
40	0.000125427	0.000116202	1311.037396

Table 4.11 (Cont.)

Normal Force (N)	a	b	Pmax [Mpa]
50	0.000135113	0.000125175	1412.272223
60	0.000143579	0.000133018	1500.763179
70	0.000151149	0.000140032	1579.893319
80	0.000158029	0.000146405	1651.803612
90	0.000164356	0.000152268	1717.944986
100	0.000170231	0.00015771	1779.351502
110	0.000175726	0.000162801	1836.789173
120	0.000180898	0.000167592	1890.843121
130	0.000185789	0.000172124	1941.971565
140	0.000190436	0.000176429	1990.540849
150	0.000194866	0.000180533	2036.849006

Assign the normal force at 40 N because the heater of micro-tribometer machine cannot generate heat much more than 150°C and the maximum velocity of tribometer can generate is 0.2 m/s. Accordingly, the minimum film thickness (h_0) from calculation is about 0.045 μm in Table 4.12. So the wear scar can generate because the surface roughness of liner specimen in Figure 4.26 is about 0.465 μm that higher than the minimum film thickness.

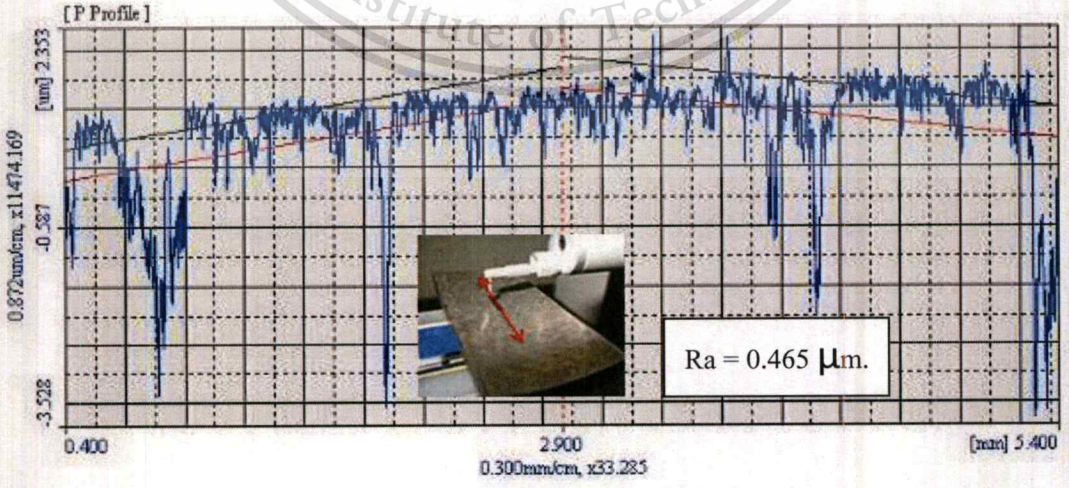

Figure 4.26 Surface roughness of liner specimen along the specimen axial direction

Table 4.12 The calculated minimum film thickness

U [m/s]	h_0/R'	h_0	h_0[μm]
0.05	5.36909E-06	1.76237E-08	0.017623704
0.1	8.60203E-06	2.82356E-08	0.028235638
0.15	1.13329E-05	3.71997E-08	0.037199719
0.2	1.37816E-05	4.52374E-08	0.045237437

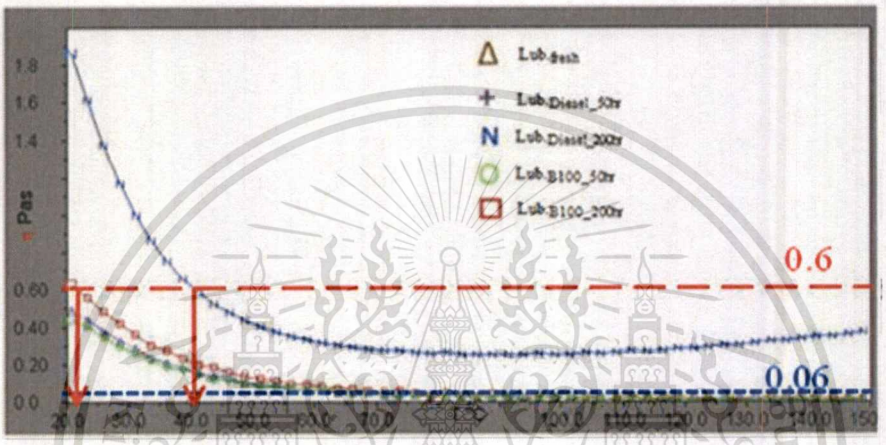

Figure 4.27 Tribometer test parameter: viscosity vs. temperature (1)

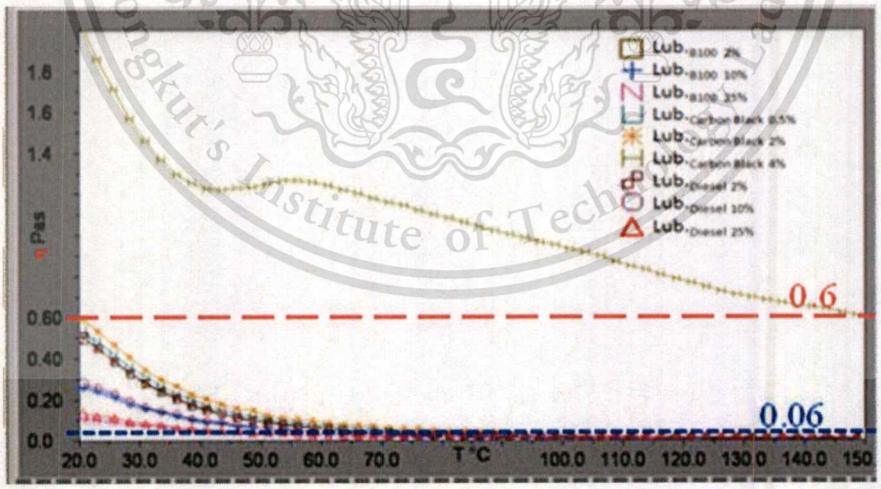

Figure 4.28 Tribometer test parameter: viscosity vs. temperature (2)

From rheometer results, the relationship between lubricant viscosity and test temperature were obtained as shown in Figure 4.27 and Figure 4.28. The constant viscosity of normal

viscosity at 0.06 Pas and high viscosity at 0.6 Pas were selected to determine the appropriate temperature for tribometer testing.

Table 4.13 The calculated tribometer test parameters for different lubricant blends

Sample Lubricant oil	Viscosity [Pas]	Temperature [°C]
Fresh Oil	0.06	60
Lub. + Diesel 2%	0.06	56
Lub. + Diesel 10%	0.06	50
Lub. + Diesel 25%	0.06	35
Lub. + B100_2%	0.06	60
Lub. + B100_10%	0.06	47
Lub. + B100_25%	0.06	34
Lub. + Carbon Black 0.5%	0.06	62
Lub. + Carbon Black 2%	0.06	70
Lub. + Carbon Black 4%	0.6	146
Lub._B100@50hr.	0.06	60
Lub._B100@200hr.	0.6	24
Lub._Diesel@50hr	0.06	60
Lub._Diesel@200hr	0.6	42

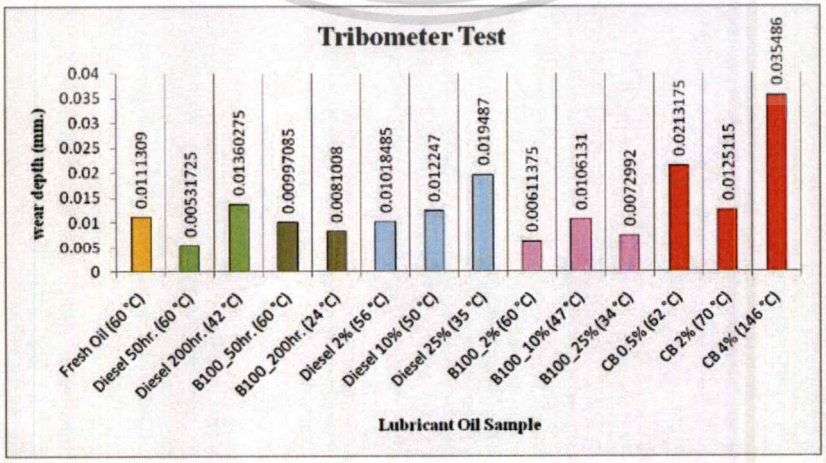

Figure 4.29 Tribometer test results from collected lubricants and batch of lubricant blends

4.5 The physical characteristics of soot from diesel-fueled engines and biodiesel-fueled engine checking by Transmission Electron Microscopy (TEM)

The average size of soot from the exhaust of diesel-fueled engine was about 20-50 nm with agglomerate, potato-shaped appearance.

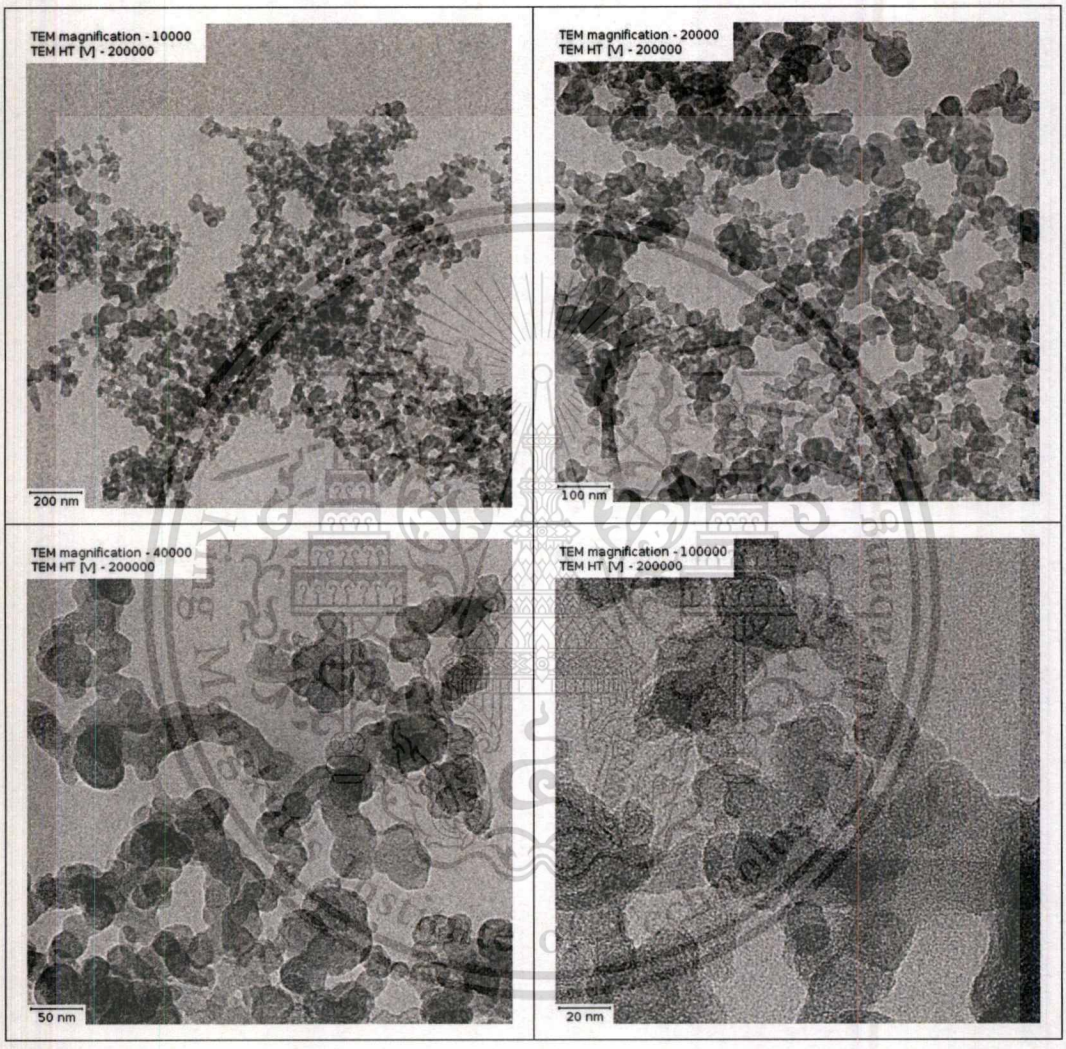

Figure 4.30 TEM images of diesel soot

The average size of soot from the exhaust of biodiesel-fueled engine was about 15-40 nm with agglomerate, potato-shaped appearance.

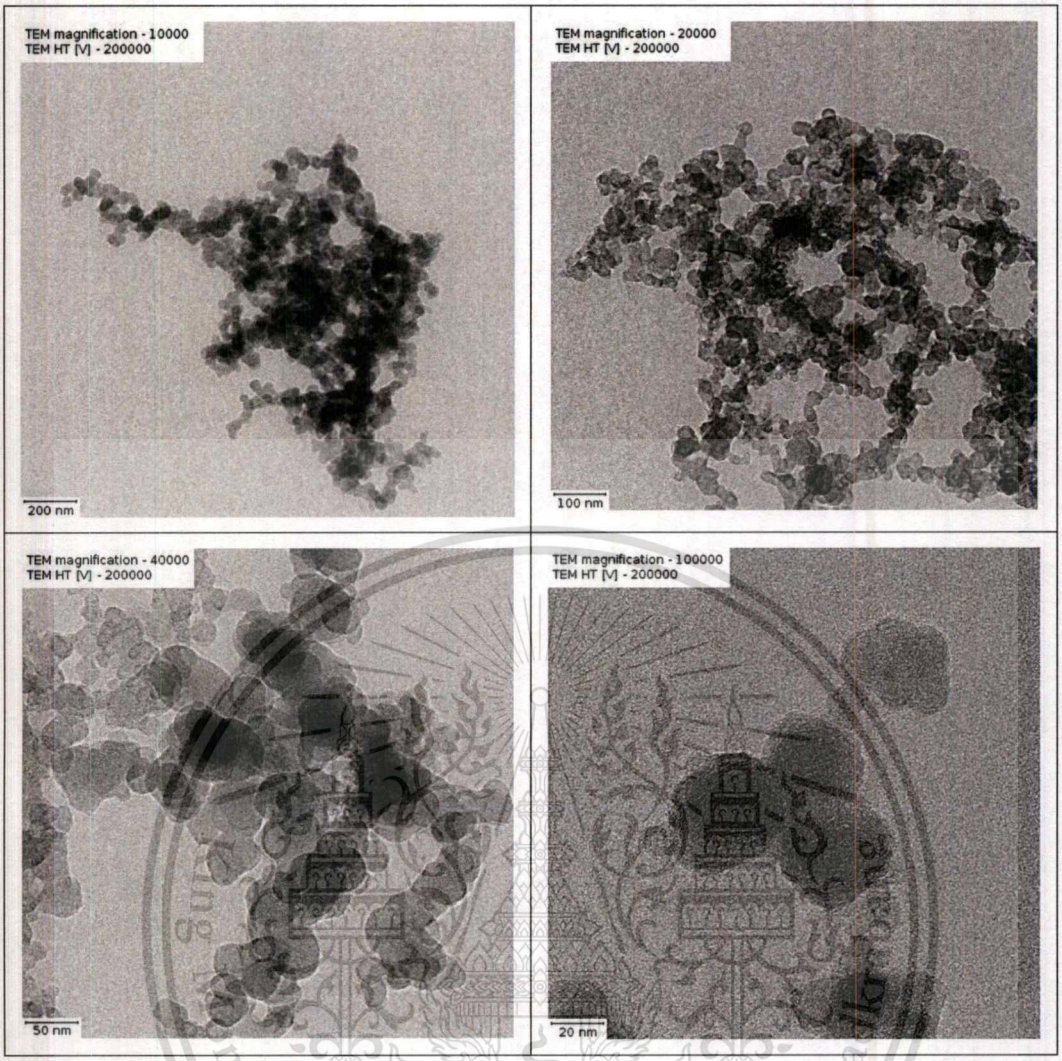

Figure 4.31 TEM images of biodiesel soot

CHAPTER 5

CONCLUSIONS

From all the experimental results on the analysis of oil samples collected from the diesel-fueled engine and biodiesel-fueled engine reported in the previous chapter, the overall summary of this study could be presented as shown in Table 5.1.

Table 5.1 Summary of results comparison from lubricant oil samples collected from the diesel-fueled engine and biodiesel-fueled engine

Lubricant	Soot	Fuel	Iron (Fe)	Viscosity
Diesel-fueled	◎	△	○	◎
Biodiesel-fueled	○	◎	◎	△
	◎ High △ Quiet low	○ Quiet high △ Low		

The impact of soot contamination on the lubricant oil viscosity was significant. The corresponding viscosity of the lubricant significantly increased with a higher soot contamination. On the other hand, it was found that the fuel contamination of used lubricant oil from biodiesel-fueled engine was higher than that of diesel-fueled engine for the same engine test period. Furthermore, the viscosity of used lubricant oil from biodiesel-fueled engine had lower viscosity when compared with used lubricant oil from diesel-fueled engine in same period operation engine. The impact of contamination by the fuel was a reduction in effective viscosity of the lubricant despite a relatively high level of soot contamination. It could be concluded that the lubricant oil contaminated with soot showed an increase in the viscosity while the lubricant oil contamination with fuel led to a decrease in the viscosity.

The contamination of the metal could be considered as an indicator of the engine wear condition. The result by ICP showed that the lubricant oil from biodiesel-fueled engine has a higher wear. It was believed that the viscosity of the lubricant at the time of testing has a major impact on the wear behavior of the engine. In diesel-fueled engine, the main contamination was

soot. As a result, the viscosity increases by the time of engine operation. Even though a higher viscosity generally means a beneficial contribution to the film formation, when the viscosity became too high, this might make the lubricant flow into the contact area more difficult. As a result, the contact area might not be properly lubricated as it should have been leading to wear in the engine parts.

In case of biodiesel-fueled engine, it was found that the lubricant was contaminated with high level of both soot and fuel (ester), especially the latter. As a result, the effective viscosity of the contaminated lubricant should increase according to the high amount of soot. However the lubricant viscosity was not as high, closer to the same range as the fresh lubricant. It was believed this was due to a presence of high fuel contamination. This could result in a better condition for lubrication purpose but it could also increase a chance of wear debris entering into the contact resulting in relatively higher wear.

On the other hand, the results from tribometer testing appeared to be inconsistent with the ICP results, especially for the lubricant oils from 200-hours test. It was possible that the collected lubricant oil was deteriorating during the middle of the engine operation. One of the main factors that has effect on the performance of lubricant is the viscosity of the lubricant. The high viscosity lubricant could make lubricant oil flowing into contact more slowly. Then the specimen and a ball steel could come into direct contact causing high wear. Furthermore, this could be due to the pressure distribution on the specimen and ball steel differed from the real engine. Additionally, in an actual engine operating condition, an engine lubrication system was a system that consisted of multiple components. Thus, the measurement of metal from ICP result could reflect a whole of the lubrication system in the engine while the tribometer test only concentrated on the contact between the piston ring and cylinder wall (liner).

Overall, all the test results from this study suggested that the use of both diesel and biodiesel could have an unfavorable effect on lubricant performance to prevent wear on engine parts. The high amount of soot contamination from diesel-fueled engine resulted in a higher lubricant viscosity, hence adversely affecting the lubricating conditions. On the other hand, even though the amount of soot contamination in the biodiesel-fueled engine was also rather high, the presence of significant biodiesel fuel contamination effectively diluted the lubricant oil, notably decreasing the resulting viscosity, hence adversely affecting the performance of the lubricant by allowing wear debris to enter the contact relatively easier. Finally, even though no definite conclusion

could be made from the current study on whether diesel or biodiesel had more negative effect on lubricant performance, it could be suggested regarding the practical aspect of biodiesel application that the lubricant change period as a maintenance protocol was shorter or more often than that of diesel-fueled engine. This was mainly due to the high fuel contamination level in the lubricant observed in this study.

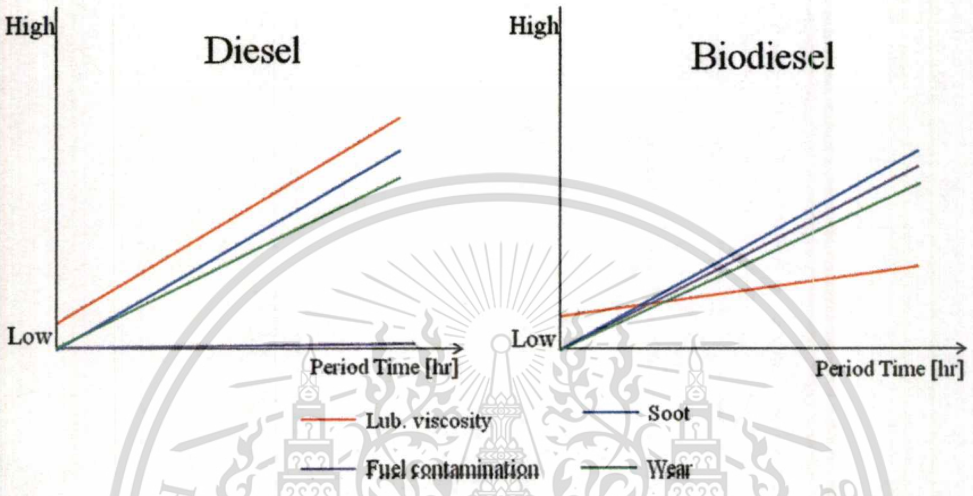

Figure 5.1 Result compare between diesel and biodiesel

REFERENCES

[1] Surapol Raadnui, and Anant Meenak, Effects of refined palm oil (RPO) fuel on wear of diesel engine components, Wear 254 (2003), 1281-1288.

[2] Sam George, Santhosh Balla and, Mridul Gautam, Effect of diesel soot contaminated oil on engine wear, Wear 262 (2007), 1113-1122.

[3] P.R. Ryason, I. Chan, J. Gilmore, Polishing wear by soot, Wear 137 (1990) 15-24.

[4] I. Berbeizer, J. Martin, P. Kapsa, The Role of Carbon in Lubricated Mild Wear, CNRS, France, 1986.

[5] Mridul Gautam, Karthik Chitoor, Murali Durbha and, Jerry C. Summers, Effect of diesel soot contaminated oil on engine wear—investigation of novel oil formulations, Tribology International 32 (1999), 687-699.

[6] Sam George, Santhosh Balla, Vishaal Gautam and, Mridul Gautam, Effect of soot on lubricant oil viscosity, Tribology International 40 (2007), 809-818.

[7] E S Yamaguchi, M Untermann, S H Roby, P R Ryason, and S W Yeh, Soot wear in diesel engines, Proc. IMechE Vol.220 Part J:J. Engineering Tribology, 463-469.

[8] S. Aldajah, O.O. Ajayi, G.R. Fenske and, I.L. Goldblatt, Effect of exhaust gas recirculation (EGR) contamination of diesel engine oil on wear, Wear 263 (2007), 93-98.

[9] Juhun Song, Mahabubul Alam, Andre L. Boehman and, Unjeong Kim, Examination of the oxidation behavior of biodiesel soot, Combustion and Flame 146 (2006), 589-604.

[10] Ming Zheng, Mwila C. Mulenga, Graham T. Reader, Meiping Wang, David S-K. Ting and, Jimi Tjong, Biodiesel engine performance and emissions in low temperature combustion, Fuel (2007).

[11] James P. Szybist, Juhun Song, Mahabubul Alam and, Andre L. Boehman, Review Biodiesel combustion, emissions and emission control, Fuel Processing Technology 88 (2007), 679-691.

[12] Allison M. Toms, Jay R. Powell, and John Dixon, The Utilization of FT-IR for Army Oil condition Monitoring, Proc. 1998 JOAP International Condition Monitoring Conference, Humphrey, G.& R. Martin, ed., JOAP-TSC, Pensacola, FL (1998), 170-176.

[13] H.H. Masjuki, and M.A. Maleque, The effect of palm oil diesel fuel contaminated lubricant on sliding wear of cast irons against mind steel, Wear 198 (1996), 293-299.

REFERENCES (CONT.)

[14] H.H. Masjuki, M.A. Maleque, A. Kubo, and T. Nonaka, Plam oil and mineral oil based lubricants-their tribological and emission performance, Tribology International 32 (1999), 305-314.

[15] Syed Ameer Basha, K. Raja Gopal, S. Jebaraj, A review on biodiesel production, combustion, emissions and performance, Renewable and Sustainable Energy Reviews 13 (2009), 1628-1634.

[16] Tze-Chi Jao, Cathy C. Devlin, C. A. Passut and R. L. Campbell, Biodiesel Fuel Effect on Diesel Engine Lubrication, Powertrains, Fuels and Lubricants Meeting, USA, 2008.

[17] Hiralal Bhowmick, S K Majumdar and S K Biswas, Tribology of soot suspension in hexadecane as distinguished by the physical structure and chemistry of soot particles, Journal of physics D: Applied physics 45 (2012)

[18] Amornsit Maan, et al. Principles and Techniques of Instrumental Analysis Spectroscopy, 1st Edition. Chulalongkorn university press, Bangkok (2010), 139-197.

[19] Gwidon W.Stachowiak and Andrew W.Batchelor, Engineering Tribology, Butterworth-Heinemann, Woburn (2001), 284-314.

APPENDIX A

ICP Testing Report

Intertek

LABORATORY ACCREDITATION TESTING No.0809

TEST REPORT

Number: BKKH10055437

Applicant: NATIONAL METAL AND MATERIALS TECHNOLOGY CENTER 114 THAILAND SCIENCE PARK PAHOLYOTHIN RD., KLONG 1, KLONG LUANG, PATHUMTHANI 12120 THAILAND
ATTN: K.PRASIT

Date: Jan 04, 2011

Sample description:

Four (4) bottlesof submitted sample said to be Used Oil
(a) one (1) bottle of Used oil (Diesel 50 hrs)
(b) one (1) bottle of Used oil (Diesel 200 hrs)
(c) one (1) bottle of Used oil (B100 50 hrs)
(d) one (1) bottle of Used oil (B100 200 hrs)

Item name: Used oil
Date sample received: December 28, 2010
Testing period: December 28, 2010 to January 04, 2011

Test conducted:

As requested by the applicant, for details please refer to attached page(s)
Type of test: Wet Chemical Analysis

Authorized by :
For Intertek Testing Services (Thailand)

Phanit Hitapong
Division Manager
Toys & Hardlines Division

Intertek Testing Services (Thailand) Limited
5/1, Phahon Yothin 28, Phahon Yothin Road, Lat Yao, Chatuchak, Bangkok 10900 Thailand
Tel.: (662) 930-6554, (662) 939-0661 Fax: (662) 939-0191
E-mail Address: tth.thailand@intertek.com

Intertek

LABORATORY ACCREDITATION TESTING No.0009

TEST REPORT

Number: BKKH10055437

Test conducted:

(A) Test result summary:

Testing item	Result (mg/kg) Submitted samples			
	(a)	(b)	(c)	(d)
Aluminium (Al) content	2	2	13	9
Chromium (Cr) content	ND	ND	ND	ND
Copper (Cu) content	ND	ND	ND	ND
Iron (Fe) content	20	39	18	62
Lead (Pb) Content	ND	ND	ND	ND
Nickle (Ni) content	ND	ND	ND	ND
Silicon (Si) content	ND	ND	ND	3
Zinc (Zn) content	189	42	159	65

Name of operation: Phanupong C.

mg/kg = Milligram per kilogram based on weight of sample = ppm
ND = Not Detected

Tested components:
(a) = Liquid (Diesel 50 hrs)
(b) = Liquid (Diesel 200 hrs)
(c) = Liquid (B100 50 hrs)
(d) = Liquid (B100 200 hrs)

(B) Test method:

Testing item	Testing method	Limit of quantification
Aluminium (Al) content	With reference to USEPA 3052:1996, by Acid digestion and determined by ICP-OES	2 mg/kg
Chromium (Cr) content	With reference to USEPA 3052:1996, by Acid digestion and determined by ICP-OES	2 mg/kg
Copper (Cu) content	With reference to USEPA 3052:1996, by Acid digestion and determined by ICP-OES	2 mg/kg
Iron (Fe) content	With reference to USEPA 3052:1996, by Acid digestion and determined by ICP-OES	2 mg/kg
Lead (Pb) Content	With reference to USEPA 3052:1996, by Acid digestion and determined by ICP-OES	2 mg/kg
Nickle (Ni) content	With reference to USEPA 3052:1996, by Acid digestion and determined by ICP-OES	2 mg/kg
Silicon (Si) content	With reference to USEPA 3052:1996, by Acid digestion and determined by ICP-OES	2 mg/kg
Zinc (Zn) content	With reference to USEPA 3052:1996, by Acid digestion and determined by ICP-OES	2 mg/kg

Remark: Reporting limit = Quantitation limit of analyte in sample
********** E N D **********/DE/SUT/KS

Intertek Testing Services (Thailand) Limited
5/1, Phahon Yothin 26, Phahon Yothin Road, Lat Yao, Chatuchak, Bangkok 10900 Thailand
Tel.: (662) 930-6554, (662) 939-0661 Fax: (662) 939-0191
E-mail Address: tth.thailand@intertek.com

Intertek

TEST REPORT

Number: BKKH11055966S2

Applicant: NATIONAL METAL AND MATERIALS TECHNOLOGY CENTER (MTEC)
114 THAILAND SCIENCE PARK, PAHOLYOTHIN RD., KLONG 1, KLONG LUANG, PATHUMTHANI 12120
ATTN: K.PRASIT

Date: Mar 10, 2011
This report supersedes the previous report date Mar 09, 2011

Sample description:

Ten (10) bottles of submitted sample said to be Used oil (Diesel 50hr.), Used oil (Diesel 200hr.), Used oil (B100 50hr.), Used oil (B100 200hr.) and Fresh oil

Item name:	Engine oil
Manufacturer name:	PTT
Date sample received:	January 17, 2011
Testing period:	January 17, 2011 to January 21, 2011

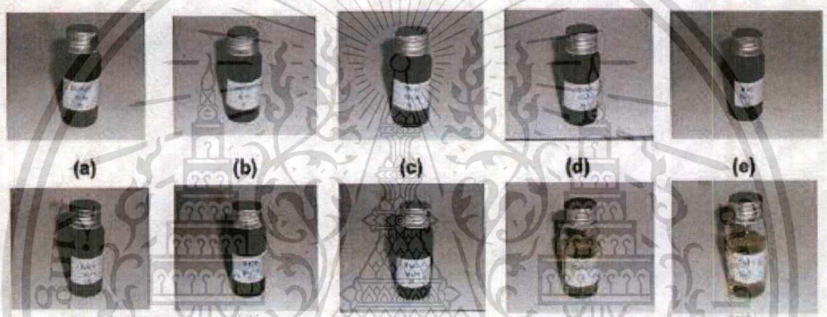

BKKH11055966S2

Test conducted:

As requested by the applicant, for details please refer to attached page(s)
Type of test: WET chemical analysis

Authorized by :
For Intertek Testing Services (Thailand)

Phanit Hitapong
Division Manager
Toys & Hardlines Division

Intertek Testing Services (Thailand) Limited
5/1, Phahon Yothin 28, Phahon Yothin Road, Lat Yao, Chatuchak, Bangkok 10900 Thailand
Tel.: (662) 930-6554, (662) 939-0661 Fax: (662) 939-0191
E-mail Address: tth.thailand@intertek.com

Intertek

TEST REPORT

Number: BKKH11055966S2

Test conducted:

(A) Test result summary:

Testing item	Result(mg/kg) Submitted samples				
	(a)	(b)	(c)	(d)	(e)
Aluminium (Al) Content	ND	ND	2	ND	3
Iron (Fe) Content	27	47	74	91	38
Silicon (Si) Content	ND	ND	ND	ND	ND
Zinc (Zn) Content	114	115	52	74	38
Phosphorus (P) Content	185	188	126	165	124

Testing item	Result(mg/kg) Submitted samples				
	(f)	(g)	(h)	(i)	(j)
Aluminium (Al) Content	4	20	9	ND	ND
Iron (Fe) Content	44	31	32	ND	ND
Silicon (Si) Content	ND	8	ND	ND	ND
Zinc (Zn) Content	26	150	160	494	534
Phosphorus (P) Content	94	282	288	296	324

Name of operation: Phanupong C.

mg/kg = Milligram per kilogram based on weight of sample = ppm
ND = Not Detected

Tested components:
(a) = Black oil (Used oil (Diesel 50 hr.) No. 1)
(b) = Black oil (Used oil (Diesel 50 hr.) No. 2)
(c) = Black oil (Used oil (B100 200hr.) No. 1)
(d) = Black oil (Used oil (B100 200hr.) No. 2)
(e) = Black oil (Used oil (Diesel 200 hr.) No. 1)
(f) = Black oil (Used oil (Diesel 200 hr.) No. 2)
(g) = Black oil (Used oil (B100 50hr.) No. 1)
(h)= Black oil (Used oil (B100 50hr.) No. 2)
(i) = Yellow liquid (Fresh oil no.1)
(j) = Yellow liquid (Fresh oil no.2)

(B) Test method:

Testing item	Testing method	Limit of quantification
Aluminium (Al) Content	With reference to USEPA 3052:1996, by Acid digestion and determined by ICP-OES	2 mg/kg
Iron (Fe) Content	With reference to USEPA 3052:1996, by Acid digestion and determined by ICP-OES	2 mg/kg
Silicon (Si) Content	With reference to USEPA 3052:1996, by Acid digestion and determined by ICP-OES	2 mg/kg
Zinc (Zn) Content	With reference to USEPA 3052:1996, by Acid digestion and determined by ICP-OES	2 mg/kg
Phosphorus (P) Content	With reference to USEPA 3052:1996, by Acid digestion and determined by ICP-OES	2 mg/kg

Remark : Reporting limit = Quantitation limit of Analyte in sample
********** E N D **********/NU/DE/KS

Intertek Testing Services (Thailand) Limited
5/1, Phahon Yothin 28, Phahon Yothin Road, Lat Yao, Chatuchak, Bangkok 10900 Thailand
Tel.: (662) 930-6554, (662) 939-0661 Fax: (662) 939-0191
E-mail Address: th.thailand@intertek.com

BIOGRAPHY

Name: Mr. Prasit Wattanawongsakun

Date of Birth: May 27, 1976

Place of Birth: Bangkok, Thailand

Education:

1997-2001	B. ME. Department of Mechanical Engineering, Faculty of Engineer, Kasetsart University
2007-2012	M. Eng. in Automotive Engineering (International program), International College, King Mongkut's Institute of Technology Ladkrabang (KMITL)

Honour and Scholarships:

2007-2009	Full scholarship for study in the master degree from National Science and Technology Development Agency (NSTDA)

Publications:

1. P. Wattanawongsakun, C. Benyajati, C. Charoenphonphanich, and K. Hidenori. "Effect of Biodiesel Combustion Product on Engine Wear Performance of Lubricant." The 7th International Conference on Automotive Engineering (ICAE-7), Bangkok, Thailand, March 28- April 1, 2011. pp 31.
2. Chatrchai Chandenduang, Narong Pitaksapsin, and Prasit Wattanawongsakun, "The Application of 3D Scanner in Reverse Engineering" Proceedings of The Third Thailand Materials Science and Technology Conference, 10 – 11 August 2004

SAE THAILAND

GPI บริษัท กรุงเทพรับ อินดัสทรี จำกัด

The 7th International Conference on Automotive Engineering

ICAE-7

Final Program & Abstracts

Green Technology for Future Vehicles

March 28 - April 1, 2011
Challenger, Impact, Muang Thong Thani,
Bangkok, Thailand

G12

Effects of Biodiesel Combustion Product on Engine Wear Performance of Lubricant

Prasit Wattanawongsakun (Graduate Student, TAIST Tokyo Tech Automotive Engineering (International Program)), (National Metal and Materials Technology Center), Chi-na Benyajati (National Metal and Materials Technology Center), Chinda Charoenphonphanich (Faculty of Engineering King Mongkut's Institute of Technology Ladkrabang), -THAILAND and Kosaka Hidenori (Tokyo Institute of Technology), -JAPAN

In this study, palm biodiesel (B100) were chosen to study an effect of biodiesel combustion product on engine wear. The tests were mainly comprised of 2 parts. In the first part, an engine was connected to a generator, which acted as a payload, and was operated according to specific testing conditions. For the other part, the lubricant oil samples obtained from each engine were collected for a qualitative wear performance study by using a ball-on-flat Micro-Tribometer. Additionally, several techniques of spectroscopy analysis were performed on the collected lubricants to study the chemical compositions as well as contaminations. The results indicated a higher wear occurred in an engine operated with biodiesel compared to the one tested with diesel. However, the lubricant obtained from an engine running with diesel displayed much more level of soot than that drained from an engine running with biodiesel.

G13

Tactile Stimulating System for Warning Purpose

Suthinanth Rattanachotithavorn, Pattarawit Sae-Ong, Witaya Wannasuphoprasit (International School of Engineering, Faculty of Engineering, Chulalongkorn University), -THAILAND

This research involves the design of the tactile stimulating system for warning purpose using the vibrating technique. The stimulation was performed on the human back area. In designing the stimulating device, the two-point discrimination experiment was done to determine the suitable stimulating positions on the back area using the stimuli with the vibrating frequency of 250 Hz. The experiment shows that human back can be stimulated at four positions. The human requires longer distances to discriminate the sense of two points of vibrating sources. The 95 percentile values of the experimental result were used in the design so that most people can use the device efficiently. Then, the prototype was designed and constructed to test the efficiency by measuring the reaction time. The distances between each stimulus were 240 mm in the vertical direction, whereas the distances in horizontal direction were 135 mm and 115 mm for the upper and lower positions respectively. The operation of stimulating device was controlled by ARM7 LPC2148 microcontroller to perform the vibrating operation and also measure the reaction time. The real reaction times of the tactile stimulation of male and female samples are 252 ms and 239 ms respectively. The comparison of reaction time among the visual, auditory, and tactile stimulating types implies that the new tactile stimulating device using vibrating technique is very efficient and suitable to be used as a reasonable alternative in stimulating application.

The 7th International Conference on Automotive Engineering (ICAE-7)
March 28 – April 1, 2011, Challenger, Impact, Muang Thong Thani, Bangkok, Thailand

Effects of Biodiesel Combustion Product on Engine Wear Performance of Lubricant

Prasit Wattanawongsakun[1,2], Chi-na Benyajati[2]

[1] Graduate Student, TAIST Tokyo Tech Automotive Engineering (International Program)
[2] Automotive laboratory, National Metal and Materials Technology Center (MTEC), Thailand

Chinda Charoenphonphanich
Faculty of Engineering King Mongkut's Institute of Technology Ladkrabang (KMITL)

Kosaka Hidenori
Tokyo Institute of Technology, Japan

ABSTRACT

In this study, palm biodiesel (B100) were chosen to study an effect of biodiesel combustion product on engine wear. The tests were mainly comprised of 2 parts. In the first part, an engine was connected to a generator, which acted as a payload, and was operated according to specific testing conditions. For the other part, the lubricant oil samples obtained from each engine were collected for a qualitative wear performance study by using a ball-on-flat Micro-Tribometer. Additionally, several techniques of spectroscopy analysis were performed on the collected lubricants to study the chemical compositions as well as contaminations. The results indicated a higher wear occurred in an engine operated with biodiesel compared to the one tested with diesel. However, the lubricant obtained from an engine running with diesel displayed much more level of soot than that drained from an engine running with biodiesel.

INTRODUCTION

One of the major causes of diesel engine wear is lubrication oil contaminated with combustion products. The combustion products usually occurred from an incomplete combustion process in an engine. In case of engine fueled by conventional diesel, one of main contaminants is soot. Various studies have been carried out to study the effect of soot on engine wear [1-6]. All the studies seemed to generally agree that the presence of soot in lubricant oil would lead to a higher wear. However, there were some disagreements regarding the mechanisms in which soot could cause higher amount of wear.

One of the proposed theories was that anti-wear additives could be absorbed by soot particles during rubbing contact resulting in depleted lubricant and hence lower wears protection performance [1]. Other theory explained that soot particle simply acted as a third body in the contact and removed a protective anti-wear film via abrasive mechanism resulting in metal-to-metal contact between engine components [3,4]. On the other hand, it was also suggested that accumulation of soot in lubricant could increase its overall viscosity i.e. thickening effect [5,6,7]. This could lead to pump ability problem in the system and hence insufficient components lubrication.

So far, majority of the work in this area have been focused on combustion product of diesel. There is still limited numbers of study on the effect of biodiesel combustion products on engine wear. In addition, currently, problem of petroleum price has become pressing issue in global scale. One of the solutions is to switch to an alternative fuel derived from agricultural products. In Thailand, a recent trend of alternative fuel has inclined towards biodiesel. A study on the effect of biodiesel combustion product on engine wear performance of lubricant is therefore attractive and necessary.

EXPERIMENTAL SETUP

ENGINE TEST SETUP

The main purpose of an engine test was to generate a used and contaminated lubricant from actual engine operation for further oil analysis and tribology test. A one-cylinder agricultural engine was chosen in this study because of good endurance and convenient access to internal parts. As shown in Figure 1, the engine was attached to a generator which, in turn, was connected to a series of spotlights which acted as a payload. The test was running for 50-hour and 200-hour periods with 7500 watt of sport lights for payload. After each test period, the lubricant was drained out for use in further tests. Two different type of fuels were tested i.e. diesel, palm biodiesel (B100).

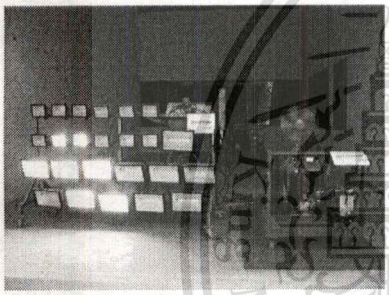

Figure 1 Engine test configuration

TRIBOMETER TEST

In order to reproduce the sliding contact conditions between liner and piston, portions of the lubricant collected from an engine test were tested on a Micro-Tribometer test machine shown in Figure 2 In this test machine, the test specimen was secured onto a lower holder stage which was filled with tested lubricant while a ball bearing was fixed to the upper holder. During the test, the upper holder would push the ball bearing against the test specimen and the lower stage would move in reciprocate direction to provide relative sliding conditions.

Test specimens were prepared by wire cutting engine liner parts of the same model as those used in the engine test along axial direction. Due to a curvature profile of the liner, specimens had to be face-milling machined on the external radius such that they could be securely placed on the lower holder stage.

General profiles of test specimen are shown in Figure 3

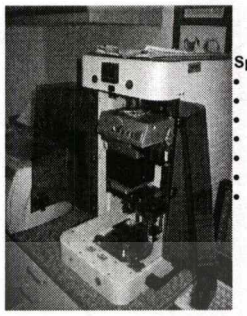

Specification

- Radius of Ball Steel 6.35 mm.
- Applied Load 200 N
- Stroke 10 mm.
- Oscillates Frequency 10 Hz
- Duration time 33 min 20 sec (400m)
- Temperature 85±3 °C
- Humidity 40-60%

Figure 2 Micro-Tribometer testing machine

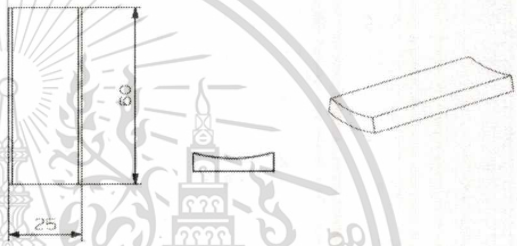

Figure 3 Test specimen for Tribometer test

LUBRICANT INSPECTIONS

The oil monitoring analysis is used for predicting the failure of engine by checking wear conditions, lubricant conditions, and contamination of lubricant. The inspection techniques employed in this study were ICPS, FT-IR, and Rheology.

Inductively Couple Plasma Spectrometer (ICPS) technique provides a spectrum of metal elements which are presented in lubricant. In other words, this technique can show how a wear condition has changed from its virgin state to its used state by compared the frequency spectrum of used oil and fresh oil [8].

Fourier Transform Infrared Spectroscopy (FT-IR) technique measures spectrum of function groups of organic elements such as water, soot, oxide and nitride products, and sulfate, etc. The contamination present in lubricant could be determined by considering area under spectrum range [9,10,11]. The measurement unit was absorbance per 0.1 mm.

Rheometer was used to measure dynamic viscosity of tested lubricants. The viscosity was measured over a temperature range of 20-150 degree Celsius. In general, this technique could be used to examine a level of lubricant degradation based on a change in viscosity.

EXPERIMENTAL RESULTS AND DISCUSSIONS

In both engine tests with biodiesel and diesel, after each specified test period of 50 hours and 200 hours, lubricant was drained out for further laboratory tests. Also, the cylinder head, piston head with rod, liner, and bearing was disassembled from the engine for a physical investigation. This also allowed replacement of new parts for a new set of test. Example of tested engine parts is shown in Figure 4 It can be seen that a piston head from the engine which had been tested for 200 hours had higher amount of soot deposit compared to the one tested for 50 hours.

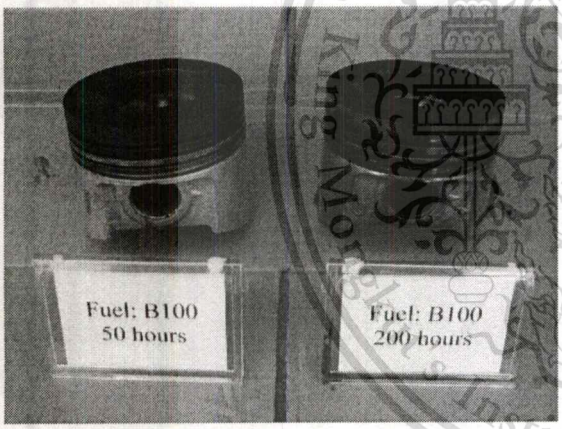

Figure 4 Piston heads after each engine test

After Tribometer testing, the specimens were cleaned by toluene followed by acetone in an ultra-sonic bathe. Then, a corresponding wear depth was determined from a wear scar profile which was obtained by using a stylus roughness measurement machine. An example of wear scar profile is illustrated in Figure 5 Additionally, specimen weight was measured prior to and after each test to estimate a resulting weight lost. The results obtained from Tribometer tests are summarized in Table 1.

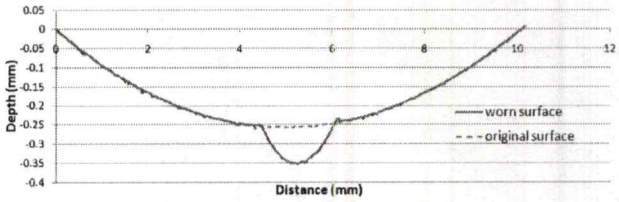

Figure 5 Example of wear depth profile by a stylus surface profiler

	No.	Wear depth (mm)	Wear depth average (mm)	Weight lost (g)	Weight lost average (g)
Fresh oil	1	0.011437	0.021170667	0.0032	0.00546
	2	0.006862		0.0058	
	3	0.045213		0.0074	
Diesel 50hr	1	0.058325	0.041796	0.0089	0.00633
	2	0.056463		0.0064	
	3	0.0106		0.0037	
B100 50hr	1	0.049188	0.029550333	0.0103	0.00793
	2	0.006925		0.0075	
	3	0.032538		0.006	
Diesel 200hr	1	0.088649	0.113266667	0.0097	0.01206
	2	0.131013		0.0143	
	3	0.120138		0.0122	
B100 200hr	1	0.089112	0.096924667	0.0082	0.00943
	2	0.110763		0.0095	
	3	0.090899		0.0106	

Table 1 Tribometer results: wear depth and specimen weight lost

It can be seen from the table above that fresh lubricant offered relatively better wear performance than other used lubricants. For tested lubricants, the ones that went through longer engine test of 200 hours gave displayed notably worse wear performance. Furthermore, for 200-hour engine test lubricants, a higher wear was observed from the lubricant collected from diesel engine test. In addition, an example of SEM image of wear scar from Tribometer test specimen is shown in Figure 6

A bar chart summarizing the ICPS results is displayed in Figure 7. Presence of iron (Fe) was detected in all lubricants collected from engine tests. However, lubricant obtained from 200-hours biodiesel engine test carried a much higher amount of iron compared to that of diesel test. Nonetheless, a phosphorus (P) level was lower in diesel case at both 50 and 200

hours test period. Similar trend were observed in level of zinc (Zn).

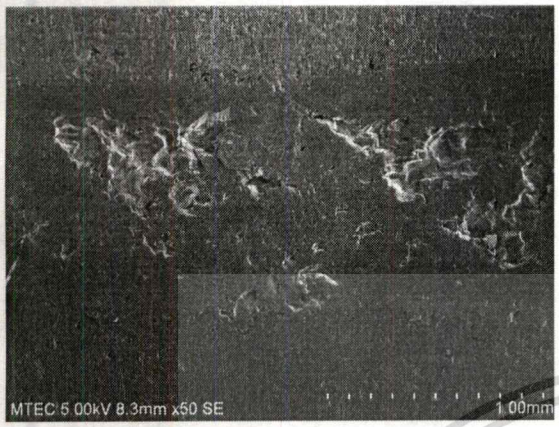

Figure 6 SEM image of wear scar on specimen after Tribometer testing

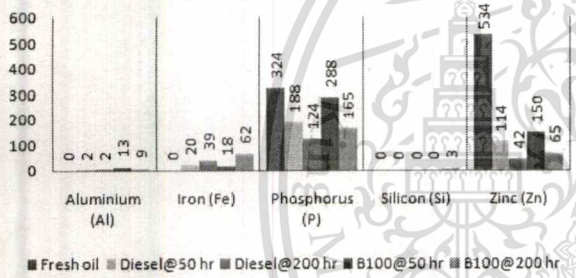

Figure 7 ICPS results of lubricants collected from different engine tests: wear condition

FT-IR results for fresh and collected lubricants are summarized in a bar chart shown in Figure 8. It can be seen that corresponding soot loading or contamination was extensively higher in lubricants running with diesel for both 50 and 200 hours engine test. However, lubricant from biodiesel engine test displayed higher contamination level for other measurements, especially oxidation.

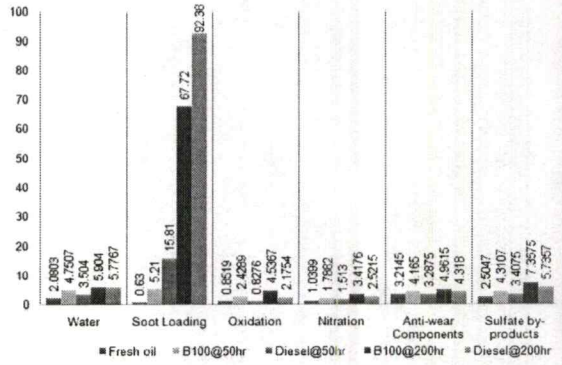

Figure 8 FT-IR results of different collected lubricants (unit: absorbance/0.1 mm)

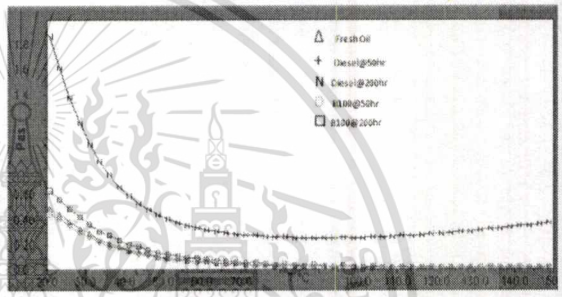

Figure 9 Viscosity measurement of collected lubricants from different engine test conditions

From oil viscosity measurement by a rheometer shown in Figure 9, generally there was only slight difference in viscosity amongst the tested lubricants. However, lubricant collected from engine tested with diesel after 200 hours exhibited a very distinct higher value of viscosity. As relatively highest level of soot contamination was detected in this particular batch of lubricant by FT-IR, this could indicate a soot thickening effect reported in literature [2, 9, 10].

By comparing the results reported in this section, there seemed to be a disagreement between qualitative wear results measured from Tribometer and actual wear results derived from lubricant analysis. Results from Tribometer showed that lubricant obtained from engine running with diesel gave rise to higher wear. On the other hand, ICPS results showed higher level of Fe iron in lubricant collected from biodiesel test run. Iron is usually associated with debris generated from wear

process. Hence, ICPS suggested the opposite of that from Tribometer.

The discrepancy could come from the limitation of Tribometer to reproduce the contact conditions that occur between piston and liner. Furthermore, wear result from an engine test might be a contribution of various tribological contacts inside the engine apart from liner wear such as bearing, gears, piston rod and pin. Hence, Tribometer results which only include wear of sliding contact between piston ring and liner might not represent the whole picture. However, the involved mechanisms which resulted in higher wear with biodiesel were still not clear.

CONCLUSIONS

In the present study, the effect of combustion product on engine wear performance of lubricant was investigated. Palm biodiesel (B100) was chosen in this study along with conventional diesel fuel. An engine test was performed to generate a used and contaminated lubricant from actual engine operation for further oil analysis and tribology test.

In tribology test using Micro-Tribometer machine, severity of wear was quantified by the depth of wear profile and total weight loss after the test. Higher wear was observed from lubricant tested for 200-hour in engine with diesel. On the other hand, wear occurred in the engine was related to the amount of iron present in the collected lubricants. In this case, it was found that higher wear occurred in an engine operated with biodiesel compared to the one tested with diesel for 200 hours engine test duration.

Further oil analysis techniques showed that the lubricant obtained from an engine running with diesel displayed much more level of soot while the lubricant drained from an engine running with biodiesel showed higher level of oxidation. Nonetheless, the responsible mechanism was still not clear. Further study is still needed.

ACKNOWLEDGMENTS

Special thanks to National Metal and Materials Technology centre (MTEC), Thailand, for funding the entire research.

REFERENCES

1. F.G. Round, Carbon: cause of diesel engine wear?, SAE 770829 (1977).
2. I. Berbeizer, J. Martin, P. Kapsa, The Role of Carbon in Lubricated Mild Wear, CNRS, France, 1986.
3. Mridul Gautam, Karthik Chitoor, Murali Durbha and, Jerry C. Summers, Effect of diesel soot contaminated oil on engine wear—investigation of novel oil formulations, Tribology International 32 (1999), 687-699.
4. P.R. Ryason, I. Chan, J. Gilmore, Polishing wear by soot, Wear 137 (1990) 15-24.
5. Sam George, Santhosh Balla and, Mridul Gautam, Effect of diesel soot contaminated oil on engine wear, Wear 262 (2007), 1113-1122.
6. Sam George, Santhosh Balla, Vishaal Gautam and, Mridul Gautam, Effect of soot on lubricant oil viscosity, Tribology International 40 (2007), 809-818.
7. E S Yamaguchi, M Untermann, S H Roby, P R Ryason, and S W Yeh, Soot wear in diesel engines, Proc. IMechE Vol.220 Part J:J. Engineering Tribology, 463-469.
8. Neramit Krasaelom, The Analyse of Wear in Single-Cylinder 4 Stroke Diesel Engine Using Liquefied Petroleum Gas as Alternative Fuel, Princess of Naradhiwas University Journal (2010)
9. Allison M. Toms, Jay R. Powell, and John Dixon, The Utilization of FT-IR for Army Oil condition Monitoring, Proc. 1998 JOAP International Condition Monitoring Conference, Humphrey, G.& R. Martin, ed., JOAP-TSC, Pensacola, FL (1998), 170-176.
10. ASTM International, Standard Practice for Used Lubricants by Trend Analysis Using Fourier Transform Infrared (FT-IR) Spectrometry, Designation: E 2412-04
11. Perkin-elmer, FT-IR Spectroscopy, Oil Condition Monitoring Using Spectrum Oil Express